SEP 24 1943

JOURNAL OF THE INSTITUTE OF PETROLEUM

FOUNDED 1913 INCORPORATED 1914

Vol. 29 AUGUST 1943 No. 236

aug 1945 24

CONTENTS

	PAGE
The Permeability of Porous Solids to Gases and Liquids. By L. Grunberg and A. H. Nissan	193
The Phase Transformations of Normal Paraffins. By C. G. Gray	226
Calibration of C.F.R. Reference Fuels. Report of Sub-Committee No. 5.—Engine Tests	235
Abstracts	291A
Book Review	315A
Books Received	316A
Institute Notes	i

Published by the Institute of Petroleum.
Address: c/o The Imperial College of Science and Technology, South Kensington, London, S.W.7.
Printed in Great Britain by Richard Clay and Company, Ltd., Bungay, Suffolk.

All rights of Publication or Translation are Reserved.

Price 7s. 6d.

THE INSTITUTE OF PETROLEUM

COUNCIL

PRESIDENT :

C. Dalley, M.I.E.E.

PAST-PRESIDENTS :

Alfred C. Adams
Lt.-Col. S. J. M. Auld, O.B.E., M.C., D.Sc.
Prof. J. S. S. Brame, C.B.E., F.I.C.
T. Dewhurst, A.R.C.S.
A. E. Dunstan, D.Sc., F.I.C.
Sir Thomas H. Holland, K.C.S.I., K.C.I.E., D.Sc., F.R.S.
J. Kewley, M.A., F.I.C.

VICE-PRESIDENTS :

Ashley Carter, A.M.I.Mech.E.
G. H. Coxon
F. H. Garner, Ph.D., M.Sc., F.I.C.
A. C. Hartley, O.B.E., F.C.G.I.
V. C. Illing, M.A.
J. A. Oriel, M.C., M.A.

MEMBERS OF COUNCIL :

R. Crichton, J.P.
A. Frank Dabell, M.I.Mech.E.
E. A. Evans, M.I.A.E.
E. B. Evans, Ph.D., M.Sc., F.I.C.
W. E. Gooday, A.R.S.M., D.I.C.
J. S. Jackson, B.Sc., F.I.C.
J. A. Oriel, M.C., M.A.
E. R. Redgrove, Ph.D., B.Sc.
C. A. P. Southwell, M.C., B.Sc.
H. C. Tett, B.Sc., D.I.C.
A. Beeby Thompson, O.B.E.
A. Wade, D.Sc., A.R.C.S.
W. J. Wilson, F.I.C., A.C.G.I.
C. W. Wood, F.I.C.

Arthur W. Eastlake, A.M.I.Mech.E.
Ashley Carter, A.M.I.Mech.E.
} Joint Honorary Secretaries

HONORARY EDITOR : Dr. A. E. Dunstan
HONORARY ASSOCIATE EDITOR : Prof. F. H. Garner, O.B.E.
HONORARY TREASURER : The Rt. Hon. Lord Plender, G.B.E.
SECRETARY : F. H. Coe

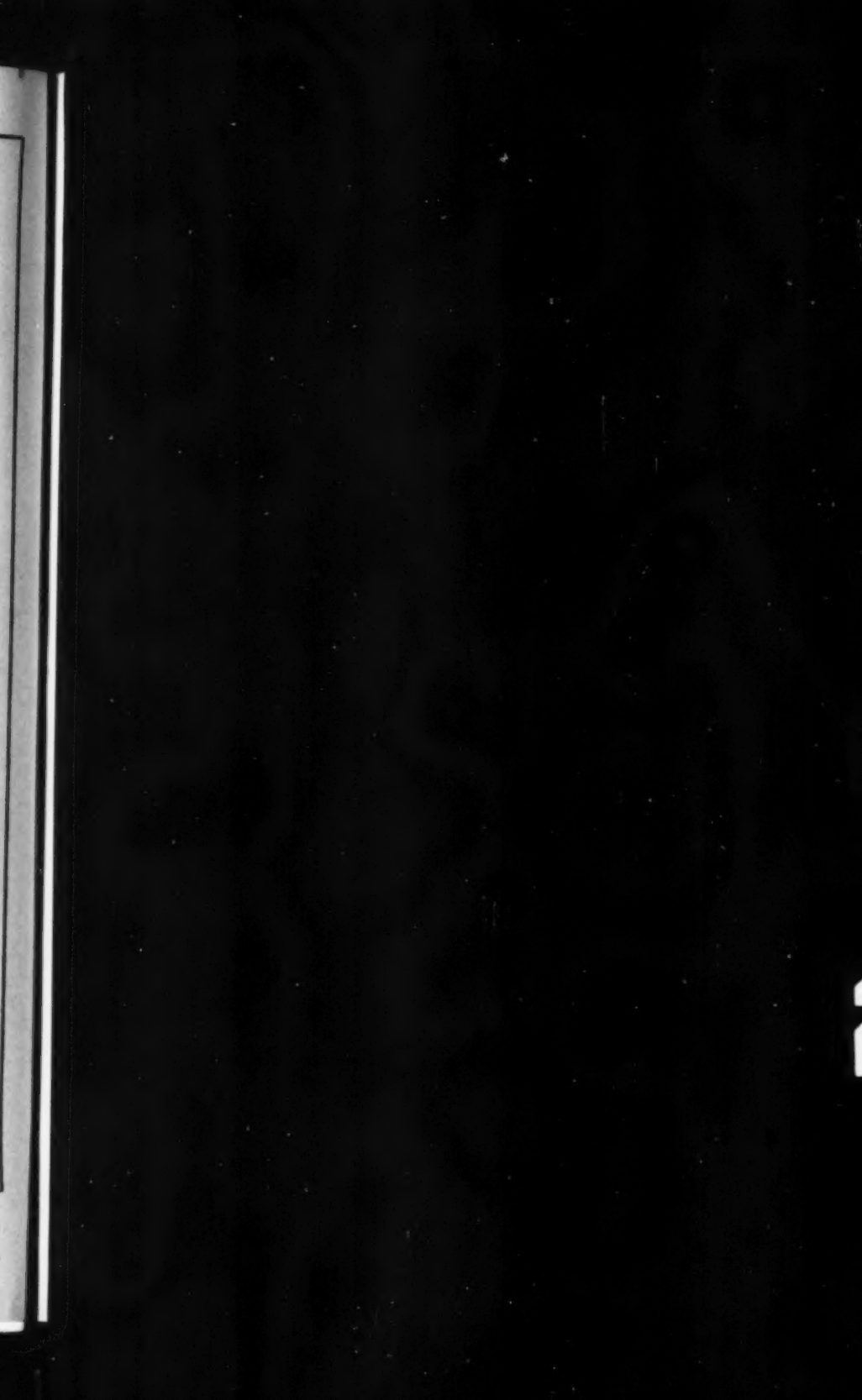

T

Ca
forma
tons/
produ
veloci
order
from
the m
exceed
advan
becom
With
the va
porou
measu
throug
exclud
introd
miner
dynam
taken
of air
difficu

Per
of liqu
virtue
of por
50–60
porosi
stated
munic

Theory

The
media,
law in

Vol. 29. No. 236. August 1943.

THE PERMEABILITY OF POROUS SOLIDS TO GASES AND LIQUIDS.*

By L. Grunberg, B.Sc., and A. H. Nissan, Ph.D.

Introduction.

Calculations reveal that the rates at which fluids flow through sand formations are extremely small. Thus an oil-well flowing, say, at 2000 tons/day from a sand 30 feet thick may be considered to be a fairly prolific producer. Yet, if the specific gravity of the oil is 0·8, the mean linear velocity at a distance of only 3 feet from the centre of the well is of the order of 0·05 cm./sec. The speed of flow is inversely proportional to distance from the well and, hence, it can be seen that in wells of more normal size the mean linear speed of the fluid in the body of the sand quickly assumes exceedingly small values. In laboratory work, however, there are advantages in maintaining fairly high rates of flow as the measurements become relatively simpler to take and the accuracy easier to maintain. With these considerations in mind, it was deemed necessary to investigate the validity of certain principles connected with the flow of fluids through porous media, when the rates of flow become very low. To attain easily measured pressure drop across the samples at low rates of flow of air through them, highly impervious samples were chosen. Liquids were excluded from the studies on rock samples for two reasons: (1) liquids introduce complex extraneous factors, such as the swelling of certain minerals, which factors may mask fundamental deviations in the hydrodynamics of the system; (2) certain measurements have already been taken by earlier workers. To obtain some relationship between the flow of air and the flow of liquids a Jena glass filter was used. In this case the difficulty mentioned above was eliminated.

Permeability is the property of porous materials, which permits the flow of liquids through these materials. A porous material is permeable by virtue of its porosity, but any attempt to express permeability as a function of porosity has failed so far. Clays, for example, having a porosity of 50–60 per cent. are practically impermeable, while sandstones with a porosity of 30 per cent. are quite permeable. However, it can be safely stated that permeability is a function of the dimensions and intercommunication of the pores, factors which in most cases cannot be determined.

Theory.

The fundamental principle governing the flow of fluids through porous media, when the flow is in the viscous region, is "Darcy's law."[1] This law in its simplest form states:

$$\frac{dp}{dx} = Cv \quad . \quad . \quad . \quad . \quad . \quad . \quad . \quad . \quad . \quad (1)$$

* Received October 30th, 1941.

where $\frac{dp}{dx}$ = pressure gradient along sample;

v = macroscopic velocity = $\frac{\text{quantity passing/unit time}}{\text{cross-sectional area}}$;

C = a constant.

The constant C contains a physical characteristic of the fluid, *i.e.*, its viscosity μ. It is usually assumed that separation of μ from the constant C frees the latter from any dependence on the nature of the fluid. In a more elaborate form Darcy's law becomes

$$K = \frac{Q\mu}{A} \cdot \frac{1}{\Delta P} \quad . \quad . \quad . \quad . \quad . \quad . \quad . \quad . \quad (2)$$

where K = permeability—*i.e.*, a characteristic of the porous medium;
Q = volumetric of flow with respect to time;
μ = viscosity of the fluid;
A = cross-sectional area of the sample;
ΔP = pressure drop per unit length.

[1] In the case of flow of gases the quantity Q is not constant, but increases with the pressure drop, according to Boyle's law, in the majority of cases. It is therefore necessary to correct this quantity, as measured at the outlet, to the mean pressure. Assuming isothermal expansion:

$$\bar{Q} = \frac{2QP_2}{P_1 + P_2} \quad . \quad . \quad . \quad . \quad . \quad . \quad . \quad (3)$$

where $\bar{Q}$ = mean quantity flowing per unit time;
$P_1 + P_2$ = absolute pressures at inlet and outlet respectively.

For gases, therefore, Darcy's law becomes:

$$K = \frac{\bar{Q}\mu}{A} \cdot \frac{1}{\Delta P} \quad . \quad . \quad . \quad . \quad . \quad . \quad . \quad . \quad (4)$$

It must, however, be pointed out that Darcy's law is, in fact, another expression of Poisseuille's law of flow through a number of capillaries:

$$Q = \frac{nR^4\pi\Delta P}{8\mu} \quad . \quad . \quad . \quad . \quad . \quad . \quad . \quad . \quad (5)$$

or

$$\frac{nR^2}{8} = \frac{Q\mu}{\pi R^2 \Delta P} \quad . \quad . \quad . \quad . \quad . \quad . \quad . \quad . \quad (6)$$

where n = number of capillaries;
R = average radius of capillaries.

Therefore

$$K = C' \times \frac{nR^2}{8}$$

where C' is a constant introduced by the fact that in Darcy's law, not the actual cross-sectional area of the capillaries through which flow is taking place, is used, but the macroscopic cross-sectional area (*i.e.*, the cross-

sectional area of the sample) and further, the cross-section of the capillaries is neither uniform nor circular.

This relationship between Darcy's and Poisseuille's laws will later be used to find the correct values of certain criteria which were found to be controlling factors of the conditions of flow.

In the c.g.s. system K is measured in darcies, when Q (or $\overline{Q}$) is measured in c.c./sec., A in cm.^{2}, μ in centipoises, and ΔP in atmosphere per centimetre length. The practical unit is the millidarcy $= 10^{-3}$ darcy.

The absolute validity of Darcy's law was challenged by early workers, who found that the quantity v did not vary linearily with $\frac{dp}{dx}$, but varied according to an exponential law. One form [2] proposed was :

$$\frac{dp}{dx} = av^n \quad . \quad . \quad . \quad . \quad . \quad . \quad . \quad . \quad . \quad (7)$$

where a and n are constants.

Another form [2] given to this equation was :

$$\frac{dp}{dx} = av + bv^2 + cv^3 \quad . \quad . \quad . \quad . \quad . \quad . \quad . \quad (8)$$

where a, b, and c are constants.

Based on an analogy with the flow of fluids through pipes, the following form is far the most popular :[1, 2]

$$\frac{dp}{dx} = av + bv^2 \quad . \quad . \quad . \quad . \quad . \quad . \quad . \quad . \quad (9)$$

where a and b are constants.

Based on the above analogy and on mathematical analysis, it is believed that for low velocities the fluid is in a state of " viscous flow," governed almost entirely by the first term of equation 9. As the velocity increases the fluid changes to a state of " turbulence " governed by the second term of equation 9. M. Muskat limits the importance of the linear term to systems with Reynolds' criterion lower than 1. The parameter for length in the criterion has hitherto been difficult to determine, so that this figure may not represent any strict limitation of the conditions under which viscous flow changes to turbulence.

Object of Investigation and Choice of Material.

As has already been mentioned, it was the object of the following investigation to test the validity of Darcy's law for rock samples, which, due to their small pore diameter, will, under test conditions, give non-turbulent flow.

Oolitic limestone was chosen, which is known to have approximately 73 per cent. of its total porosity in the form of micropores, with an equivalent diameter smaller than 0·005 mm. The results were to be correlated by tests on limestone, magnesium limestone, fine (siltstone-like) sandstone, and coarse (well-cemented) sandstone. The impervious samples were used to yield extremely low rates of flow, whilst the relatively permeable sandstones were used to correlate low and high rates in one system.

A Jena glass filter (commercial specification 11G3) was used to correlate the flow of air and of aqueous solutions and to study the permeability to liquids of different surface tensions.

Experimental Work on Gas Flow.

The cores were cut by means of a special cutter, and whenever necessary subjected to Soxhlet extraction, according to a standard procedure.[4] The dimensions of each sample were taken by means of a micrometer graduated in millimetres. Length and diameter were measured in five different planes, and the mean of five readings taken. The results are given in Table I.

Table I.

Sample.	Lithological species.	Length, cm.	Diameter, cm.	Cross-sectional area, cm.^{2}.
1	Oolite	3·1936	2·9533	6·8500
2	Oolite	3·1991	2·9656	6·9074
3	Oolite	3·1916	2·9528	6·8478
4	Oolite	3·1996	2·9728	6·9411
5	Limestone	3·2536	2·8589	6·4192
6	Very fine sandstone	1·9684	3·1003	7·5491
7	Mg. limestone	3·0304	2·8390	6·3258
8	Coarse sandstone	2·3879	2·9563	6·8799
9	Coarse sandstone	2·3499	2·9668	6·9130

The samples were thoroughly dried for 6 hours at about 70° C., and always kept in a desiccator over calcium chloride. The sample was placed in the special sample holder, and air under pressure passed through. Keeping the pressure constant, measurements were taken simultaneously for: barometric pressure, temperature, inlet and outlet pressures and rate of flow.

Special precautions were taken to keep the sample in a state of dryness throughout the experiment, firstly by passing the air through a calcium chloride container, and secondly by interposition of calcium chloride tubes whenever there was communication to measuring instruments containing water.

Apparatus.

The apparatus (Fig. 1) may be sub-divided into three sections:

(1) Source of pressure and sample holder;
(2) Pressure-measuring section;
(3) Flow-measuring section.

(1) Air under pressure from a compressor passes through two reducer valves (RV_1 and RV_2) and two pressure tanks (PT_1 and PT_2) into a calcium chloride container (CC_1). The latter also holds the thermometer (Th), which measures the temperature of the stream of air. Passing through a filter of cotton-wool, the air goes through a T-piece to the sample holder and to the pressure-measuring section.

The sample holder (*SH* and Fig. 1A) consists of a steel container and different brass tubes and rings. Rubber packings are provided to prevent any possible leakage. This holder has the advantage that a constant check on the possibility of leakage can be maintained simply by covering the top part with water, or putting the whole in a water-bath, the temperature of which can be accurately measured. If the holder is of brass, troubles of oxidation and rusting which result in the case of iron holders can be avoided.

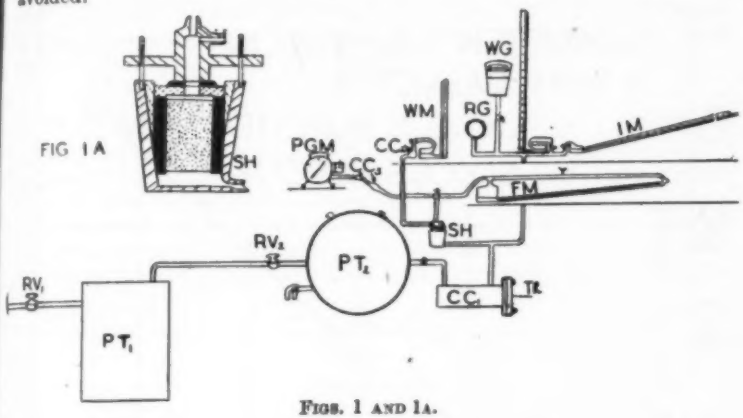

FIGS. 1 AND 1A.

(2) For the measurement of inlet pressure, the following set of gauges and manometers was provided :

(*a*) Rough gauge (*RG*) for the rough estimation of pressure.

(*b*) Calibrated Alex. Wright metal gauge (*WG*), for pressures from 130 to 300 cm. Hg.

(*c*) A straight mercury manometer (*MM*), for pressures from 25 to 130 cm. Hg.

(*d*) A manometer (*IM*) with an inclination of 1 in 4, for pressures from 0 to 25 cm. Hg.

Outlet preasure was measured by means of a water manometer (*WM*), separated by a calcium chloride tube (CC_2) from the sample holder.

(3) Up to rates of flow of 1 c.c./sec. a calibrated flowmeter (*FM*) was used, consisting of a resistance to flow (*r*), represented by a capillary of 0·1 cm. diam. and an inclined (1 in 10) toluene manometer.

Higher rates of flow were measured by means of a Parkinson gasmeter (*PGM*) and a stopwatch. The gasmeter gave one revolution for 0·5 l. gas. It was separated from the sample holder by a calcium chloride tube (CC_3).

To make the measurements on the glass filter the whole sample holder was replaced by the glass filter which was connected to the apparatus in an appropriate way.

CALIBRATIONS.

(1) The Alex. Wright metal gauge was calibrated against a mercury manometer and the calibration checked for hysteresis.

All the readings were converted into true values by means of a chart.

(2) The Parkinson gasmeter was found to read correctly for 2 l. of air, which were collected under water, and for 4 l. which were displaced from a standard flask by water.

(3) Calibration of the flowmeter was carried out for the two purposes:

(*a*) To ascertain that the flow of air through the flowmeter within the required range was viscous, as already calculated by ascertaining

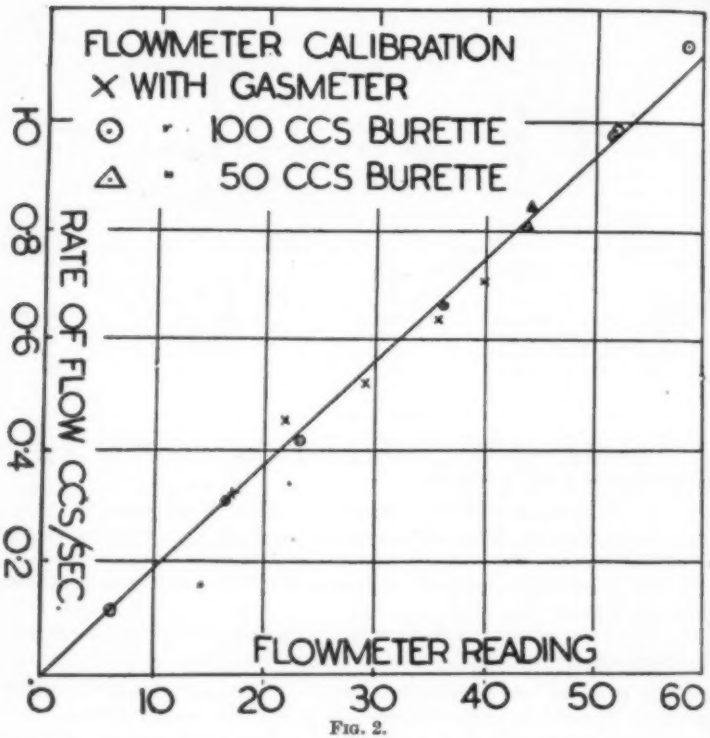

FIG. 2.

the Reynolds' number for the maximum rate of flow to be measured by the flowmeter.

(*b*) To obtain the equivalence of the flowmeter readings in c.c./sec. Calibration was first carried out by means of the gasmeter, and then by means of a 200-c.c. burette, which was filling with water from a constant pressure head, acting across a fine jet, while the air so displaced was passed through the flowmeter.

At the end of the investigation the calibration was verified by means of a 50-c.c. burette, collecting the air, issuing from the flowmeter, under water. In all cases the time was taken by means of a stopwatch. The calibration is shown graphically on Fig. 2.

Corrections.

Rate of flow as measured by the apparatus was in all cases converted to $\overline{Q}$, for considerations already given.

Whenever measurements of air were taken in contact with water the appropriate correction for water-vapour pressure at test temperature was applied—*i.e.*, the volume was reduced by the partial volume of water-vapour. This was considered necessary, because only dry air came in contact with the sample. When the dry air comes in contact with water, it becomes saturated with water-vapour, so that considerations of partial pressure and volume cannot be neglected.

Results.

In order that recalculations, or the introduction of corrections deemed necessary by other workers but neglected by the authors, may be possible, Table II gives the complete calculations sheet for one series of measurements taken on sample 1. The next tables give only the final results for one of the samples. The results for the rest of the samples may be seen from their respective figures. (The Jena glass gave Fig. 4 and rock samples Figs. 5 to 13.)

Table II.

Sample I.

Series 1. Barometer : 74·955 cm. Hg.
Viscosity of air : 0·01773 cp.
Temp. : 12·9° C. ± 0·1° C.

Inlet press., cm. Hg.	Flow-meter reading.	P_1, atm.	P_2, atm.	Q, c.c./sec.	$\overline{Q}$, c.c./sec.	$P_1 - P_2$, atm.	$\frac{\overline{Q}}{A} \times 10^3$.	$k\Delta P$, $\frac{\text{atm.}}{\text{cm.}}$
196·5	6·05	3·5718	0·9864	0·1128	0·04870	2·5854	12·60	0·8100
193·0	5·93	3·5258	0·9864	0·1106	0·04830	2·5394	12·52	0·7960
188·4	5·74	3·4658	0·9863	0·1070	0·04730	2·4795	12·25	0·7860
184·5	5·57	3·4138	0·9863	0·1038	0·04650	2·4275	12·04	0·7610
181·5	5·44	3·3738	0·9863	0·1012	0·04580	2·3855	11·87	0·7490
165·4	4·77	3·1658	0·9862	0·0881	0·04190	2·1796	10·85	0·6820
160·0	4·55	3·0918	0·9862	0·0850	0·04100	2·1056	10·61	0·6600
153·8	4·34	3·0080	0·9862	0·0810	0·03990	2·0226	10·33	0·6340
149·5	4·15	2·9558	0·9862	0·0774	0·03870	1·9696	10·03	0·6170
144·4	3·98	2·8868	0·9862	0·0741	0·03780	1·9006	9·78	0·5960
140·4	3·84	2·8358	0·9861	0·0717	0·03700	1·8497	9·68	0·5800
133·4	3·58	2·7438	0·9861	0·0670	0·03540	1·7577	9·16	0·5510
130·5	3·46	2·7048	0·9861	0·0643	0·03440	1·7187	8·90	0·5380
116·3	2·96	2·5178	0·9861	0·0550	0·03100	1·5317	8·03	0·4800
108·8	2·74	2·4178	0·9860	0·0510	0·02960	1·4318	7·66	0·4490
103·2	2·54	2·3448	0·9860	0·0472	0·02790	1·3588	7·22	0·4250
97·9	2·42	2·2748	0·9860	0·0450	0·02720	1·2888	7·05	0·4040
92·7	2·24	2·2058	0·9860	0·0418	0·02590	1·2198	6·71	0·3820
86·0	2·09	2·1208	0·9860	0·0391	0·02480	1·1348	6·42	0·3560
82·4	1·95	2·0688	0·9860	0·0362	0·02340	1·0828	6·06	0·3400
75·7	1·77	1·9818	0·9859	0·0331	0·02200	0·9959	5·70	0·3120
70·0	1·64	1·9068	0·9859	0·0307	0·02090	0·9209	5·41	0·2880
64·8	1·47	1·8388	0·9859	0·0275	0·01920	0·8529	4·97	0·2670
64·5	1·46	1·8348	0·9859	0·0273	0·01910	0·8489	4·95	0·2660
58·1	1·32	1·7508	0·9859	0·0249	0·01790	0·7649	4·64	0·2400
52·8	1·19	1·6808	0·9859	0·0222	0·01640	0·6949	4·25	0·2180
47·6	1·05	1·6123	0·9859	0·0197	0·01500	0·6264	3·88	0·1965
42·4	0·94	1·5443	0·9859	0·0178	0·01380	0·5584	3·58	0·1750
37·2	0·84	1·4733	0·9858	0·0158	0·01270	0·4895	3·29	0·1535
33·4	0·74	1·4253	0·9858	0·0141	0·01160	0·4395	3·01	0·1380
28·8	0·64	1·3648	0·9858	0·0120	0·01000	0·3790	2·59	0·1190
25·2	0·59	1·3173	0·9858	0·0111	0·00950	0·3315	2·46	0·1040
20·9	0·44	1·2608	0·9858	0·0083	0·00730	0·2750	1·89	0·0862
14·9	0·29	1·1819	0·9858	0·0058	0·00528	0·1961	1·37	0·0615
12·7	0·26	1·1530	0·9858	0·0050	0·00461	0·1672	1·19	0·0524
10·7	0·23	1·1267	0·9858	0·0044	0·00411	0·1409	1·06	0·0441

The Flow of Aqueous Solutions.

The Jena glass filter was used for two purposes:

(1) To study the flow of aqueous solutions and to establish if possible the relationship between the flow of gases and that of liquids.

(2) To measure the average pore diameter and the number of pores, so as to assign the correct value for the parameter of length in the criteria governing flow.

The apparatus used is shown on Fig. 3. It represents an ordinary flow-measuring apparatus, and is characterized by a constant-temperature control.

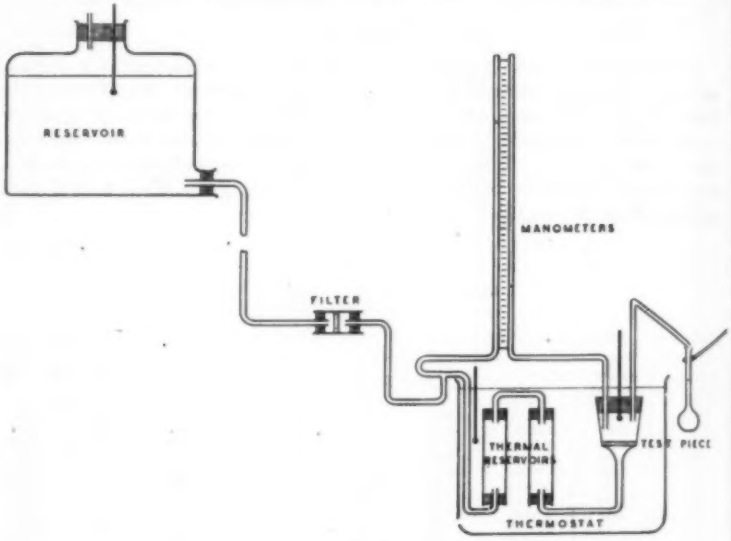

Fig. 3.

Four solutions were tested: (1) distilled water, (2) 2 per cent. *n*-amyl alcohol solution, (3) two sodium chloride solutions (0·960 and 0·614 N). The choice of these solutions was made so as to observe the influence of surface forces on the flow of liquids through porous media. Fig. 14 shows that the flow under test was non-turbulent. A certain deviation of individual results from the straight-line law can be observed.

Measurement of Pore Diameter and Calculation of the Number of Pores of the Jena Glass Filter.

The measurement of the pore radii was made according to the "bubble-pressure method" as developed by Cantor, Bechold, and others. This method is based on the following principle:

If a liquid, A, filling a capillary is subjected to the pressure of air, of a gas or a liquid B, immiscible with A, then the pressure required to displace

liquid A from the capillary must be equal or slightly higher than the pressure caused by the interfacial tension of the two phases across the curved meniscus. There is a definite relationship between the pressure required, p, the radius of the capillary, R, and the interfacial tension, σ. This relationship may be expressed by :

$$R = \frac{2\sigma}{p} \quad . \quad . \quad . \quad . \quad . \quad . \quad . \quad . \quad (10)$$

The Jena filter was saturated with a liquid of known surface tension, and pressure by air was then applied. The break-through pressure was

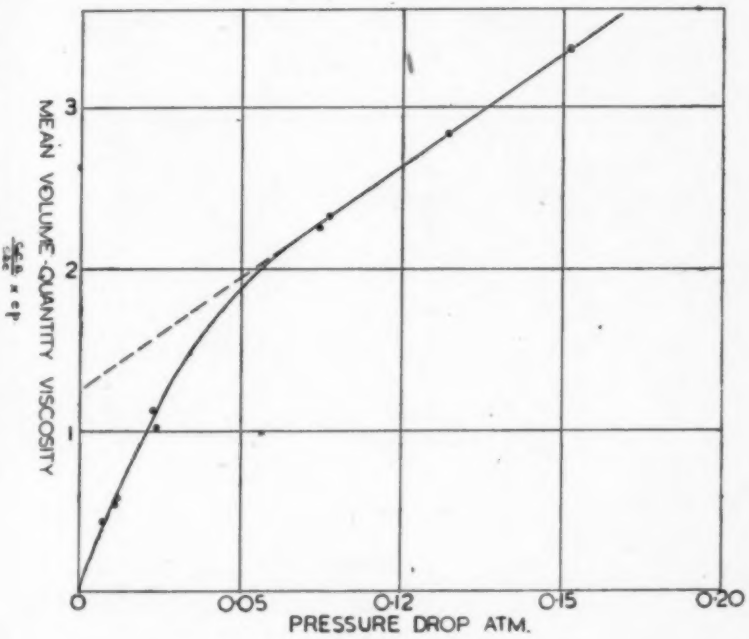

FIG. 4.

FLOW OF AIR THROUGH JENA GLASS FILTER.

observed, together with the number of capillaries through which flow of air took place—*i.e.*, capillaries having approximately equal pore radii. The experiments revealed that the variation in pore diameter was very small. All except thirty-two pores had radii between 1·0 to 1·2 $\times$ 10^{-3} cm.

Substituting a value of 10^{-3} for the pore radius in Poisseiulle's formula (equation 5), n, the number of capillaries, could be ascertained, and it was found to be 1·4 $\times$ 10^{5} as an average of several experiments using different liquids. (This gives the equivalent *circular* pores. The assumption of circularity constitutes a severe weakness in the calculations but is made

for expediency, as (1) no other method is known, and (2) the calculations are of secondary rather than primary importance in the present work.)

The quantity flowing through a single capillary, and hence the actual (not the macroscopic) mean linear velocity in the different experimental results for the flow of air through the Jena glass filter, could be calculated.

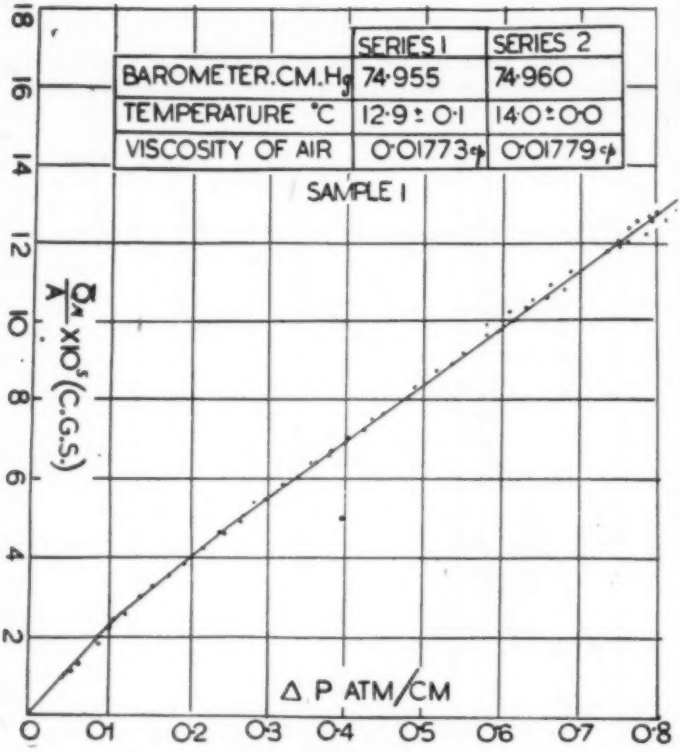

FIG. 5.

DISCUSSION ON THE FLOW OF AIR.

In all cases the plot of rate of flow *vs.* pressure drop yielded curves passing through the origin, but not in a single case could the test results be represented by a single straight line passing through the origin. As the regime was certainly sub-turbulent, these anomalies (on the basis of Darcy's law) assume significance which has to be elucidated.

Before considering the anomalies, it is well to study possible sources of systematic or accidental errors which may have given rise to the apparent anomalies. The barometer was recently checked, and found accurate, and the thermometer was calibrated against N.P.L. thermometers, and found

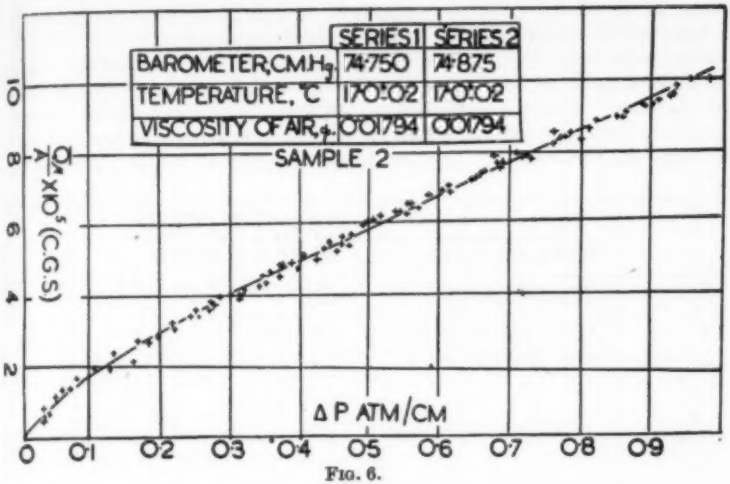
SERIES 1
SERIES 2
BAROMETER, CM. Hg. 74·750 74·875
TEMPERATURE, °C. 17·0±·02 17·0±·02
VISCOSITY OF AIR, η 0·01794 0·01794
SAMPLE 2
Q/A × 10⁵ (C.G.S.)
Δ P ATM/CM
0 0·1 0·2 0·3 0·4 0·5 0·6 0·7 0·8 0·9
2 4 6 8 10

FIG. 6.

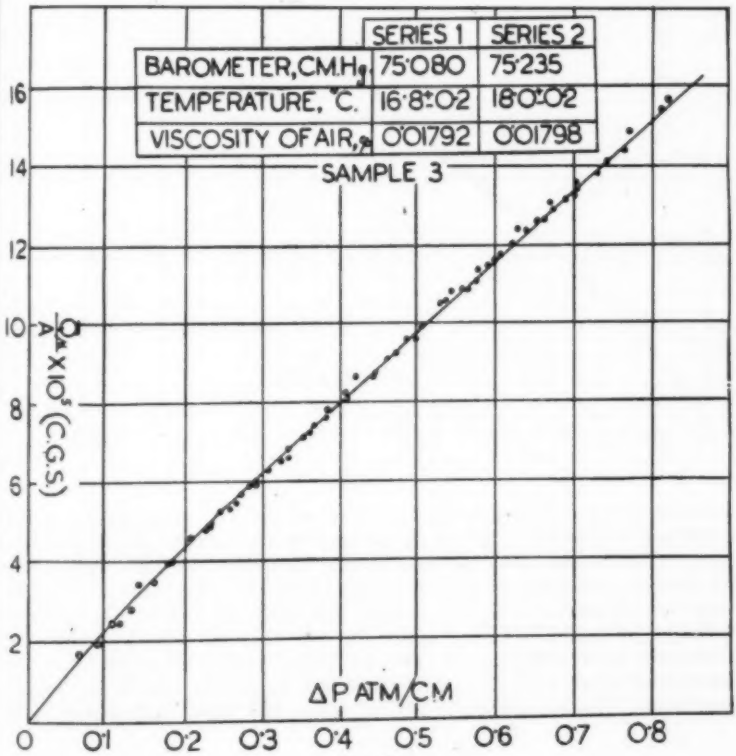
SERIES 1
SERIES 2
BAROMETER, CM. Hg. 75·080 75·235
TEMPERATURE, °C. 16·8±·02 18·0±·02
VISCOSITY OF AIR, η 0·01792 0·01798
SAMPLE 3
Q/A × 10⁵ (C.G.S.)
Δ P ATM/CM
0 0·1 0·2 0·3 0·4 0·5 0·6 0·7 0·8
2 4 6 8 10 12 14 16

FIG. 7.

accurate to $\pm 0{\cdot}05°$ C. The viscosity of air was taken from the literature, whilst the variation in it due to variation of temperature is seen from the tables to be negligible. The manometric section of the apparatus is of an absolute type, except the steel gauge, which was calibrated against a mercury manometer. That the anomalies are not due to errors in pressure measurements is shown by the fact that although the pressure range (see Table II) covered all three instruments, no break is apparent in the curve at the

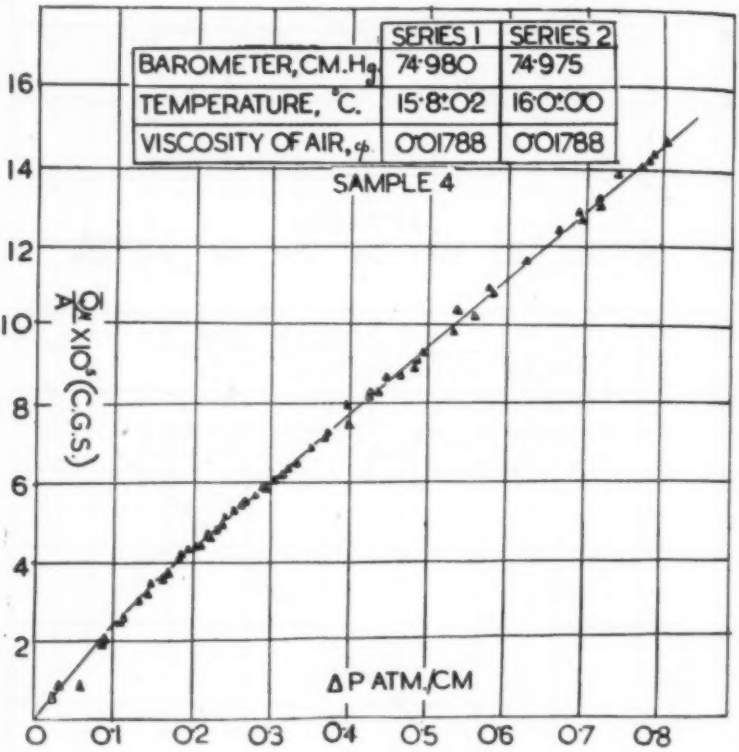

FIG. 8.

point of change from one instrument to another. The discontinuity on the curve appears to be in the range covered by the vertical mercury manometer. The usual precautions regarding verticality of scale, cleanliness of mercury, constancy of zero point, etc., were, of course, taken. The last piece or apparatus is the flowmeter, and this was calibrated by three different methods, in two of which dry air was first passed through the flowmeter, and later measured, either by the gasmeter or a burette, and in the other of which air was first measured in a burette and then displaced through the meter. As the curve on Fig. 2 shows, the three calibrations agree

well, although the first two were made before the investigation, and the last after the termination of all these studies. The stopwatch was checked against radio signals over a period of 3 hours. Thus it is concluded that, whilst errors due to instrumental inexactitudes are there, these cannot be the cause of the apparent anomalies.

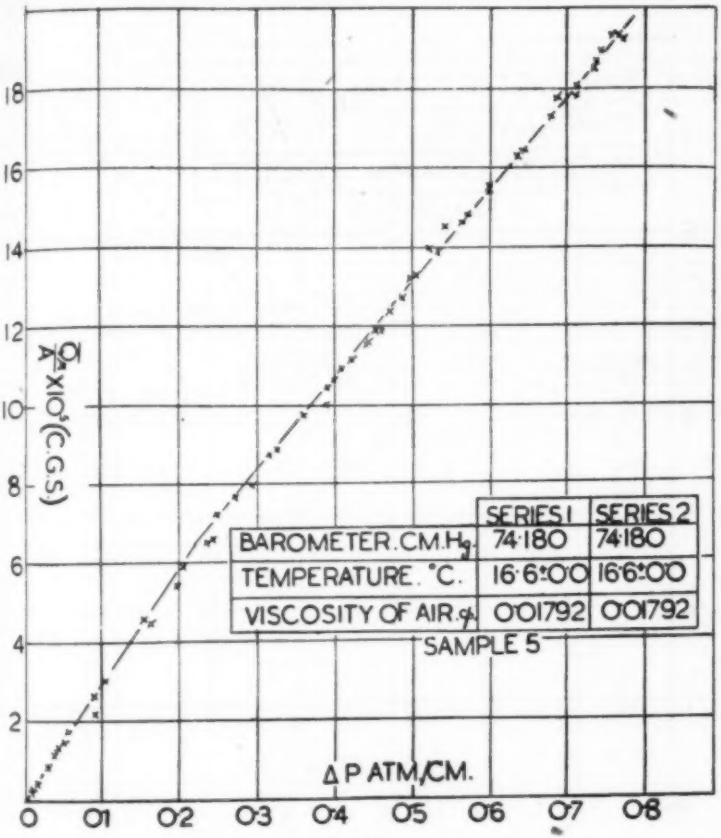

FIG. 9.

Another possible cause for the anomalies may be the method of calculation and corrections introduced or neglected. Thus, the assumption of isothermal expansion may not be correct. It is felt that the facts that the temperatures of the air inside the tank and in the laboratory were substantially the same and the small pressure drops at which the anomalies appear, justify such an assumption. Further, adiabatic expansion, if it existed, would have resulted in an apparent *increase* in permeability at higher rates of flow, instead of the *decrease* shown.[5] Again, deviations

from Boyle's law at the pressures used are negligible for air. Again, the broad policies involved in the method may be questioned. Foremost in this section is the possible condensation of water-vapour on expansion. Whilst the air used was not tested for complete dryness, it was felt that passing it through the calcium chloride dryer, 6 cm. in diameter and 16 cm. in length, at the slow rates involved in the regions exhibiting the anomalies,

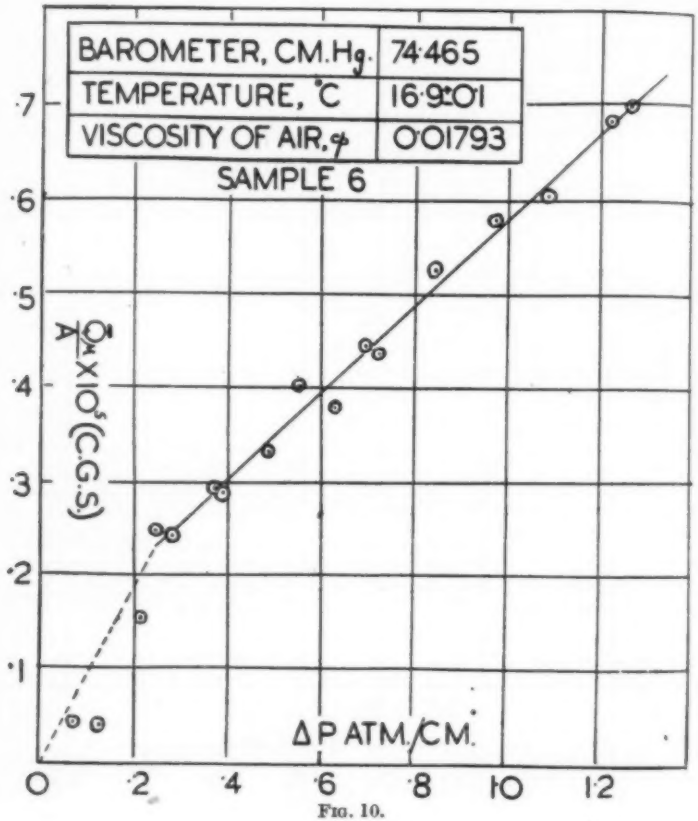

FIG. 10.

would completely eliminate this source of error. No access of water-vapour to the sample through back vapour pressure was allowed. Again, the possibility of plugging by solid particles was investigated by the several repetitions of the measurements going over the high- as well as the low-pressure differential range (see Table III). Constant check against the possibility of leakage was maintained as a matter of routine. Thus it was concluded that the anomalies exhibited in these tests were not fortuitious, but represented fundamental characteristics of the systems studied. To

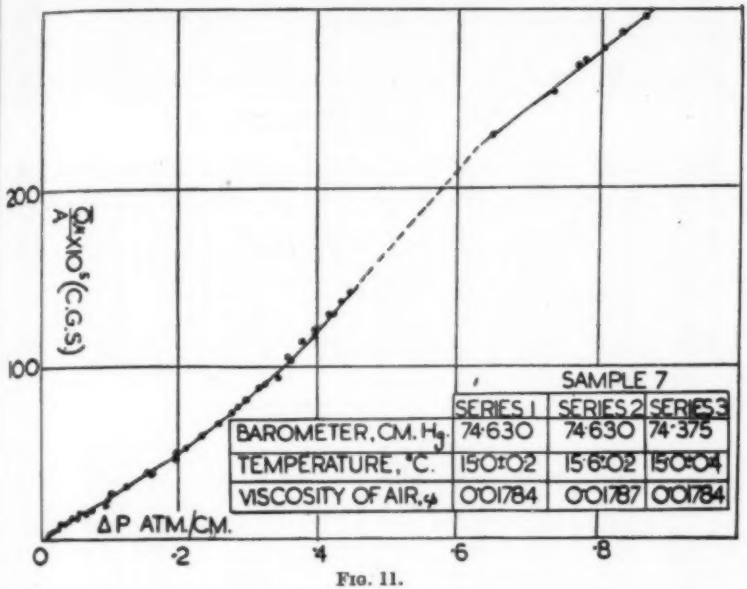
200
100
0
·2
·4
·6
·8
$\frac{Q}{A}$×10⁵(C.G.S)
ΔP ATM./CM.
SAMPLE 7
SERIES 1 | SERIES 2 | SERIES 3
BAROMETER, CM. Hg. | 74·630 | 74·630 | 74·375
TEMPERATURE, °C. | 15·0±0·2 | 15·6±0·2 | 15·0±0·4
VISCOSITY OF AIR, η | 0·01784 | 0·01787 | 0·01784

FIG. 11.

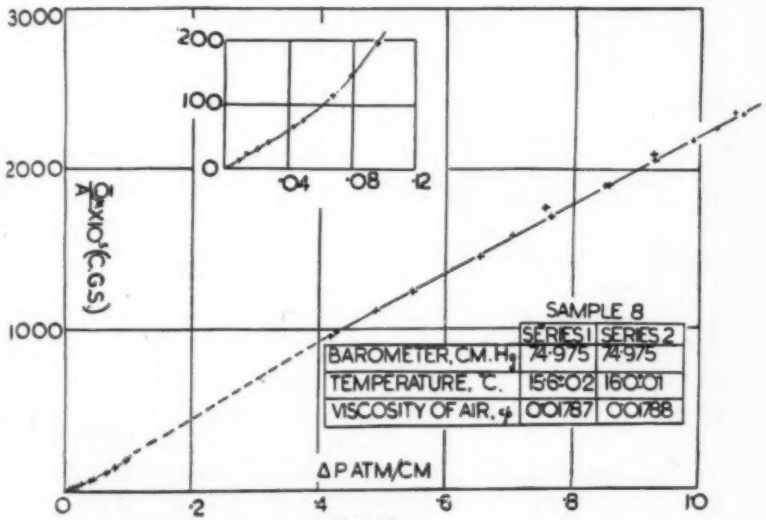
3000
2000
1000
0
·2
·4
·6
·8
10
200
100
0
·04
·08
·12
$\frac{Q}{A}$×10⁵(C.G.S)
ΔP ATM/CM
SAMPLE 8
SERIES 1 | SERIES 2
BAROMETER, CM. Hg. | 74·975 | 74·975
TEMPERATURE, °C. | 15·6±0·2 | 16·0±0·1
VISCOSITY OF AIR, η | 0·01787 | 0·01788

FIG. 12.

TABLE III.

Sample 7.

Q_1, c.c./sec.	$\overline{Q}$, c.c./sec.	$P_1 - P_2$, atm.	$\frac{\overline{Q}\mu}{A} \times 10^6$.	ΔP, $\frac{\text{atm.}}{\text{cm.}}$	Q, c.c./sec.	$\overline{Q}$, c.c./sec.	$P_1 - P_2$, atm.	$\frac{\overline{Q}\mu}{A} \times 10^6$.	ΔP, $\frac{\text{atm.}}{\text{cm.}}$
			Series 1.	Barometer: 74·630 cm. Hg. Viscosity of air: 0·01784 cp. Temp.: 15·0° C. ± 0·2° C.					
0·0817	0·07220	0·2601	20·380	0·08590	0·0256	0·02460	0·0828	6·940	0·02735
0·0631	0·05710	0·2090	16·100	0·06900	0·0231	0·02220	0·0723	5·980	0·02385
0·0504	0·04660	0·1630	13·130	0·05390	0·0194	0·01880	0·0617	5·300	0·02035
0·0343	0·03260	0·1103	9·200	0·03650	0·0149	0·01450	0·0461	4·090	0·01522
0·0237	0·02280	0·0750	6·430	0·02475	0·0115	0·01130	0·0342	3·190	0·01130
0·0160	0·01560	0·0487	4·400	0·01610	0·00907	0·00906	0·0290	2·560	0·00958
0·0117	0·01150	0·0355	3·245	0·01172	0·00741	0·00740	0·0210	2·090	0·00694
0·00704	0·00703	0·0184	1·982	0·00606	0·00520	0·00519	0·0157	1·460	0·00518
0·00464	0·00463	0·0119	1·304	0·00393	0·00409	0·00409	0·0105	1·150	0·00347
0·0683	0·06140	0·2207	17·300	0·07290	0·000925	0·000925	0·0013	0·2610	0·00043
0·0640	0·05890	0·1735	16·600	0·05730	0·0601	0·05470	0·1947	15·430	0·06430
0·0479	0·04430	0·1551	12·500	0·05120	0·0557	0·05100	0·1800	14·380	0·05940
0·0468	0·04350	0·1498	12·260	0·04950	0·0484	0·04470	0·1578	12·600	0·05210
0·0445	0·04150	0·1446	11·700	0·04770	0·0430	0·04010	0·1418	11·300	0·04680
0·0378	0·03560	0·1236	10·030	0·04080	0·0328	0·03100	0·1134	8·750	0·03740
0·0344	0·0326[illegible]	0·1117	9·190	0·03680	0·0293	0·02800	0·0946	7·900	0·03120
0·0302	0·02880	0·0973	8·120	0·03210					
			Series 2.	Barometer: 74·630 cm. Hg. Viscosity of air: 0·01784 cp. Temp.: 15·0° C[illegible] ± 0·2° C.					
0·8510	0·5050	1·3585	142·40	0·4480	0·2050	0·1595	0·5619	45·00	0·1958
0·8030	0·4820	1·3127	136·00	0·4340	0·1620	0·1310	0·4701	36·90	0·1551
0·7460	0·4550	1·2590	128·30	0·4160	0·1290	0·1080	0·3863	30·40	0·1273
0·6750	0·4210	1·1944	118·80	0·3950	0·0982	0·0835	0·3024	23·60	0·1000
0·6190	0·4060	1·1367	114·40	0·3750	0·7560	0·0835	1·2730	129·40	0·4210
0·5590	0·3700	1·0770	104·30	0·3560	0·6800	0·4220	1·1994	119·00	0·3960
0·4910	0·3260	1·0033	92·00	0·3420	0·5640	0·3640	1·0820	102·70	0·3580
0·4650	0·3120	0·9684	86·00	0·3200	0·4600	0·3090	0·9626	87·10	0·3180
0·4040	0·2780	0·8918	79·40	0·2945	0·3660	0·2570	0·8390	72·50	0·2770
0·3820	0·2660	0·8579	75·00	0·2830	0·2830	0·2080	0·7054	58·60	0·2330
0·3260	0·2340	0·7732	66·00	0·2550	0·2280	0·1740	0·6037	49·10	0·1993
0·2810	0·2070	0·7025	58·40	0·2320	0·1660	0·1340	0·4771	37·80	0·1574
0·2450	0·1850	0·6346	52·10	0·2090	0·1100	0·0952	0·3094	26·90	0·1020
			Series 3.	Barometer: 74·375 cm. Hg. Viscosity of air: 0·01784 cp. Temp.: 15·0° C. ± 0·4° C.					
2·135	0·9550	2·3392	269·00	0·7700	2·512	1·050	2·6191	296·00	0·8630
2·172	0·9650	2·3592	272·00	0·7780	1·986	0·916	2·2243	255·50	0·7350
2·270	0·9900	2·4391	279·00	0·8050	1·681	0·820	1·9673	231·00	0·6495
2·380	1·020	2·5191	288·00	0·8310					

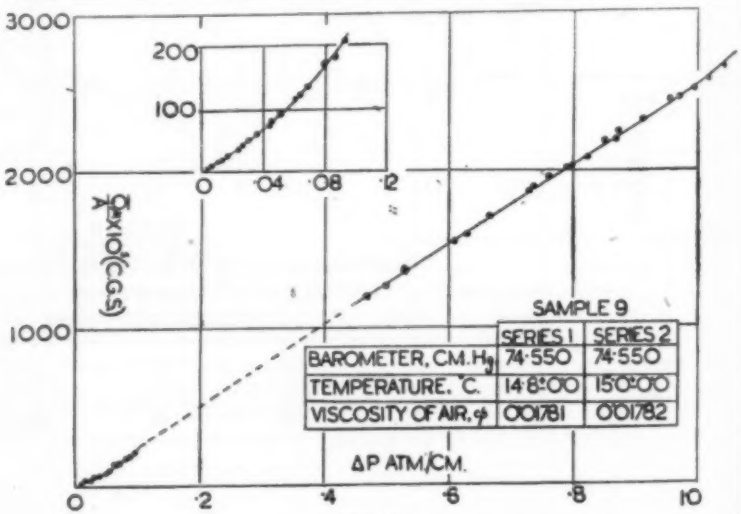

FIG. 13.

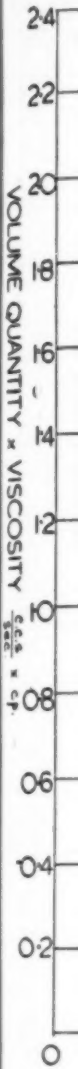

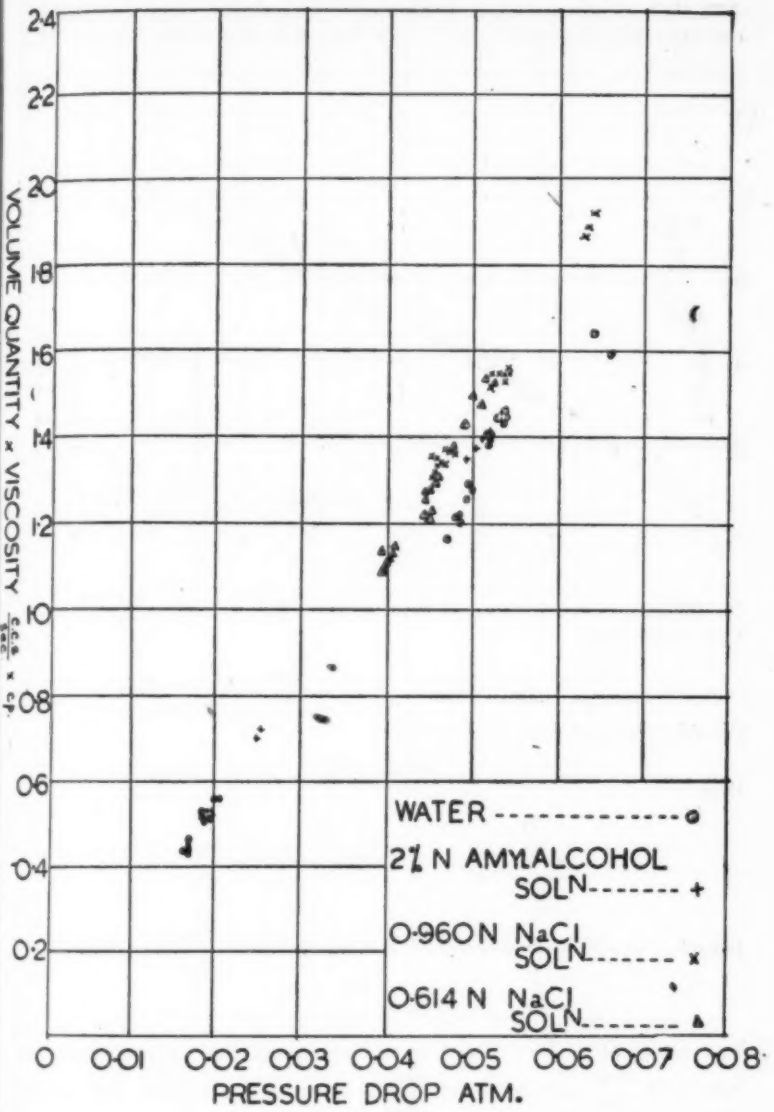

FIG. 14.

FLOW OF AQUEOUS SOLUTIONS THROUGH JENA GLASS FILTER.

show that porous materials of the same permeability range are yielding approximately the same curve, a plot was made of samples 1–5 (Fig. 15).

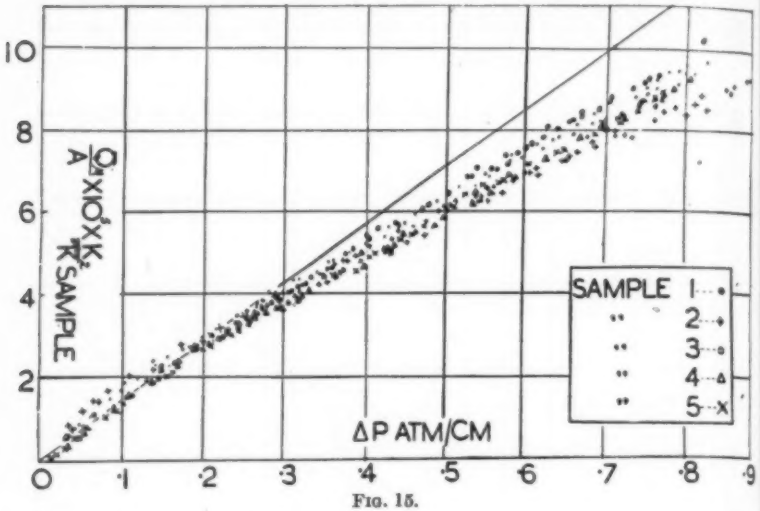

FIG. 15.

To obtain a scale which would superimpose all these curves the following was considered:

$$\frac{Q_1\mu_1}{A_1} \times \frac{1}{\Delta P_1} = K_1 \qquad \frac{\bar{Q}_2\mu_2}{A_2} \times \frac{1}{\Delta P_2} = K_2$$

Considering equal pressure drops

$$\Delta P_1 = \Delta P_2$$

then

$$\frac{\frac{\bar{Q}_1\mu_1}{A_1}}{\frac{\bar{Q}_2\mu_2}{A_2}} = \frac{K_1}{K_2} \quad \text{or} \quad \frac{\bar{Q}_1\mu_1}{A_1} = \frac{\bar{Q}_2\mu_2}{A_2} \times \frac{K_1}{K_2}$$

Sample 2 was taken as a standard, and for each point $\frac{\bar{Q}\mu}{A}$ was reduced to

$$\frac{\bar{Q}\mu}{A} \times \frac{K_2}{K \text{ sample}}$$

The values of K were taken as the average of those corresponding to $\Delta P = 0{\cdot}3 \frac{\text{atm.}}{\text{cm.}}$ and $\Delta P = 0{\cdot}8 \frac{\text{atm.}}{\text{cm.}}$. It can easily be seen that for all these samples a change in permeability occurs at approximately $\Delta P = 0{\cdot}2 \frac{\text{atm.}}{\text{cm.}}$.

Table IV gives the necessary data for this plot.

TABLE IV.

Sample No.	K at $\Delta P = 0{\cdot}8$, darcies $\times 10^{-5}$.	K at $\Delta P = 0{\cdot}3$, darcies $\times 10^{-5}$.	Average K, darcies $\times 10^{-5}$.	$\frac{K_2}{K \text{ sample}}$.
1	15·92	18·35	17·13	0·7500
2	10·79	13·35	12·07	1·0000
3	19·10	20·85	19·88	0·6500
4	18·26	20·26	19·26	0·6300
5	25·30	27·40	26·35	0·4580

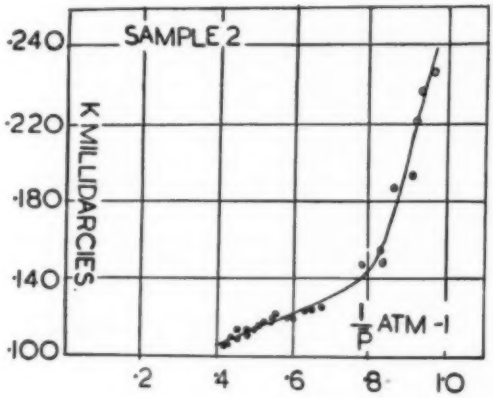

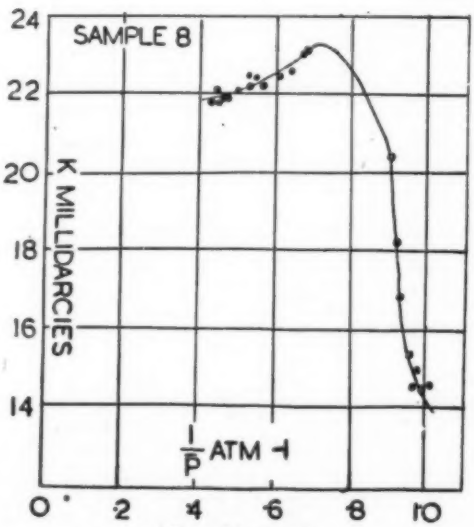

FIGS. 16 AND 17.

Corresponding data for samples 6–9 are given in Table V.

TABLE V.

Sample No.	K at $\Delta P = 0{\cdot}8$, darcies $\times 10^{-3}$.	K at $\Delta P = 0{\cdot}3$, darcies $\times 10^{-3}$.	Average K, darcies $\times 10^{-3}$.	$\frac{K_3}{K \text{ sample}}$
6	0·625	0·867	0·796	15·1630
7	354·0	263·5	308·75	0·0391
8	2224·0	2272·0	2248·0	0·00537
9	2530·0	2600·0	2565·0	0·00471

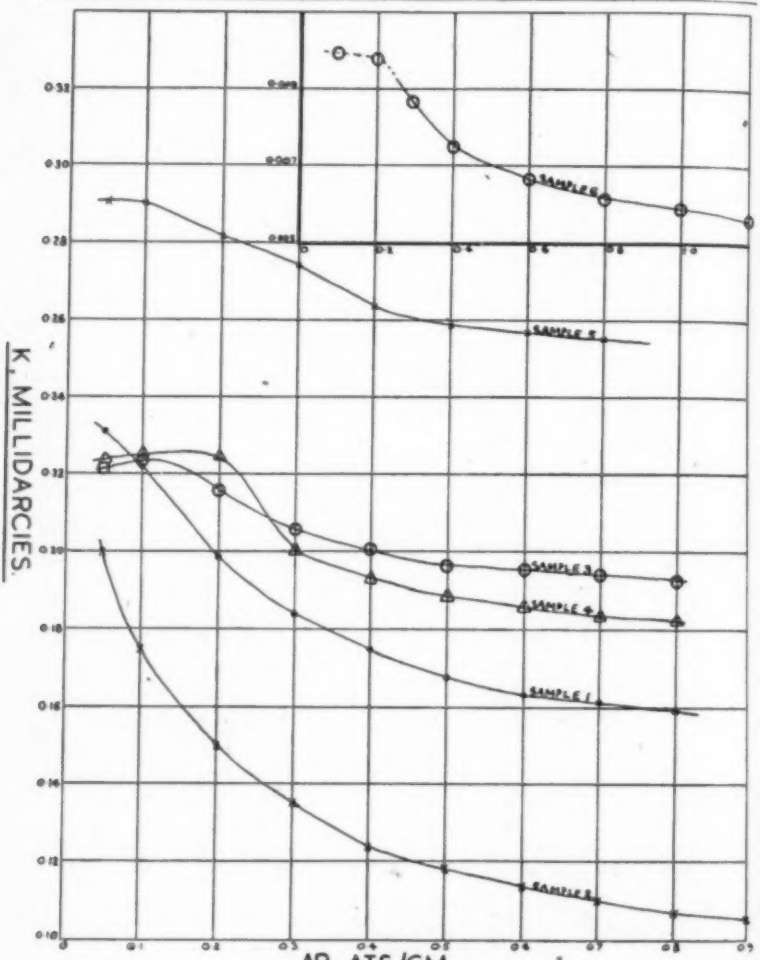

FIG. 18.

An attempt was made to investigate the experimental results from the point of view of the mean free-path theory put forward by Klinkenberg.[6] This theory proposes that the permeability of porous media to gases is a linear function of the reciprocal of the mean pressure, but not a function

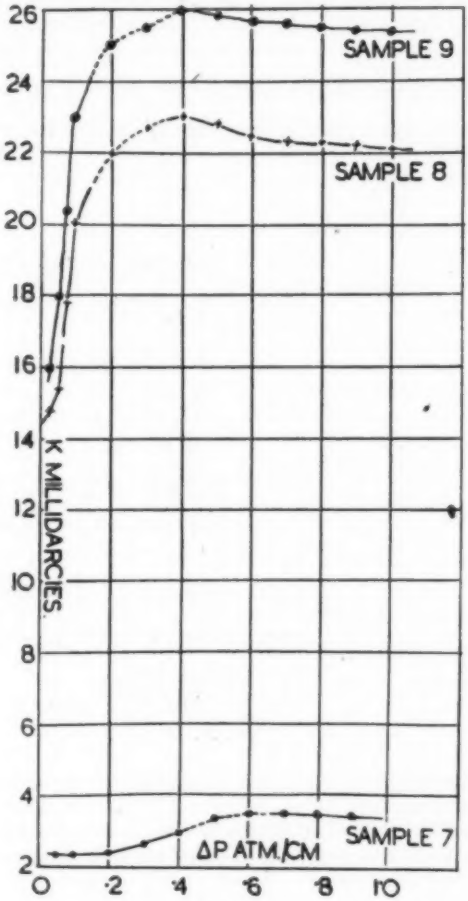

FIG. 19.

of the pressure drop. In plotting K *vs.* $\frac{1}{P}$ a straight line should be obtained, which, when extrapolated to zero—*i.e.*, infinite mean pressure—should give the permeability of the material to liquids. This method of plotting was adopted, but, as Figs. 16 and 17 show, no straight line was obtained. The curves obtained are actually the mirror images of the curves K *vs.* ΔP, as shown on Figs. 18 and 19. By plotting some of Klinkenberg's results

as K *vs.* $P_1 - P_2$ (*i.e.*, the equivalent of ΔP (Fig. 20)), it was observed that there was some relationship between the variation of permeability and the pressure drop. For very small values of pressure drop an increase of permeability with pressure drop becomes evident, while at greater values a straight line is obtained, which straight line may correspond to the assymptotic part of the curves obtained in the present work.

The tests on the Jena glass, which was of the same type as those used by Klinkenberg, did not result in a definite curve when K *vs.* $\frac{1}{\bar{P}}$ were plotted. Under certain conditions the permeability of air was lower than that to

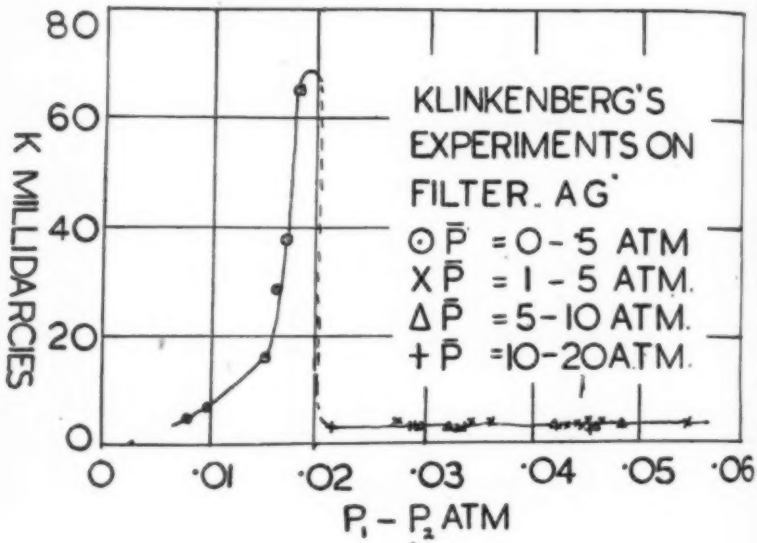

FIG. 20.

liquids, which is difficult to explain on the slip theory connecting permeability and the mean pressure.

To bring out the true relationships in these contradictory results, it was considered necessary to apply dimensional analysis to the various factors, which might be fundamental. Thus:

$$f(K, \bar{P}, \Delta P, v, D, \rho, \mu) = 0 \quad . \quad . \quad . \quad . \quad . \quad (11)$$

where D = average diameter of the capillaries;
ρ = density of the gas;

while the notation of the other factors remains as previously given. The different dimensionless functions were determined and tested for validity.

Buckingham's π Theorem [7] had to be employed, as the number of factors exceeded five. The functions obtained were:

$\pi_1 = \left(\frac{K}{D^2}\right)$, which is in accordance with the definition of the coefficient of permeability;

$\left.\begin{aligned}\pi_2 &= \frac{\bar{P}}{\rho v^2}\\ \pi_3 &= \frac{\Delta P}{\rho v^2}\end{aligned}\right\}$ functions which will have to be tested on the experimental results;

$\pi_4 = \frac{\mu}{vD\rho}$, Reynolds' criterion, which has always been considered as one of the chief controlling factors.

Hence the equation becomes:

$$f\left[\left(\frac{K}{D^2}\right), \left(\frac{\bar{P}}{\rho v^2}\right), \left(\frac{\Delta P}{\rho v^2}\right), \left(\frac{\mu}{vD\rho}\right)\right] = 0 \quad . \quad . \quad . \quad (12)$$

or

$$K = CD^2 f\left[\left(\frac{\bar{P}}{\rho v^2}\right), \left(\frac{\Delta P}{\rho v^2}\right), \left(\frac{\mu}{vD\rho}\right)\right]$$

$$= C' f\left[\left(\frac{P}{\rho v^2}\right), \left(\frac{\Delta P}{\rho v^2}\right), \left(\frac{\mu}{vD\rho}\right)\right] \quad . \quad . \quad . \quad . \quad (13)$$

where C and C' are constants.

Considering the density and pressure at which volume measurements were taken:

ρa = density of air at atmospheric pressure;
Pa = atmospheric pressure;
va = velocity at atmospheric pressure;
Qa = volume quantity flowing per unit time at atmospheric pressure,

$$K = C' f\left[\left(\frac{\bar{P}}{\frac{\rho a \bar{P}}{Pa} \times \frac{va^2 Pa^2}{\bar{P}^2}}\right), \left(\frac{\Delta P}{\frac{\rho a P}{Pa} \times \frac{va^2 Pa^2}{\bar{P}^2}}\right), \left(\frac{\mu}{vD\rho}\right)\right]$$

$$= C' f\left[\left(\frac{\bar{P}^2}{\rho a Pa va^2}\right), \left(\frac{\Delta P \times P}{\rho a Pa va^2}\right), \left(\frac{\mu}{vD\rho}\right)\right]$$

which can be written as:

$$K = C\left[\phi_1\left(\frac{\bar{P}^2}{Qa^2}\right), \phi_2\left(\frac{\Delta P \times \bar{P}}{Qa^2}\right), \phi_3\left(\frac{\mu}{vD\rho}\right)\right] \quad . \quad . \quad (14)$$

since $(\rho a Pa) =$ constant and $Qa^2 =$ constant $\times va^2$.

If $\phi_1\left(\frac{\bar{P}^2}{Qa^2}\right)$ and $\phi_2\left(\frac{\Delta P \times \bar{P}}{Qa^2}\right)$ affect the value of K fundamentally, they will give definite curves on plotting K *vs.* function, while if this is not the case, a spread of the points will be observed. In other words, the true relationship between K and $\bar{P}$ and between K and ΔP will be shown plotting K *vs.* the two dimensionless functions obtained, and not *vs.* $\bar{P}$ or ΔP alone. Figs. 21, 22, and 23 show the application of these considerations to the experimental results of samples 2, 7, and 8. The functions are not shown for the other samples, as the three samples shown typify the others.

Sample 2 (Fig. 21) shows that the permeability coefficient K is a function of $\frac{\bar{P}^2}{Qa^2}$ over the whole range of the curve, while K is a function of $\left(\frac{\Delta P \times \bar{P}}{Qa^2}\right)$ over a limited range only. The two functions where any curve is obtainable

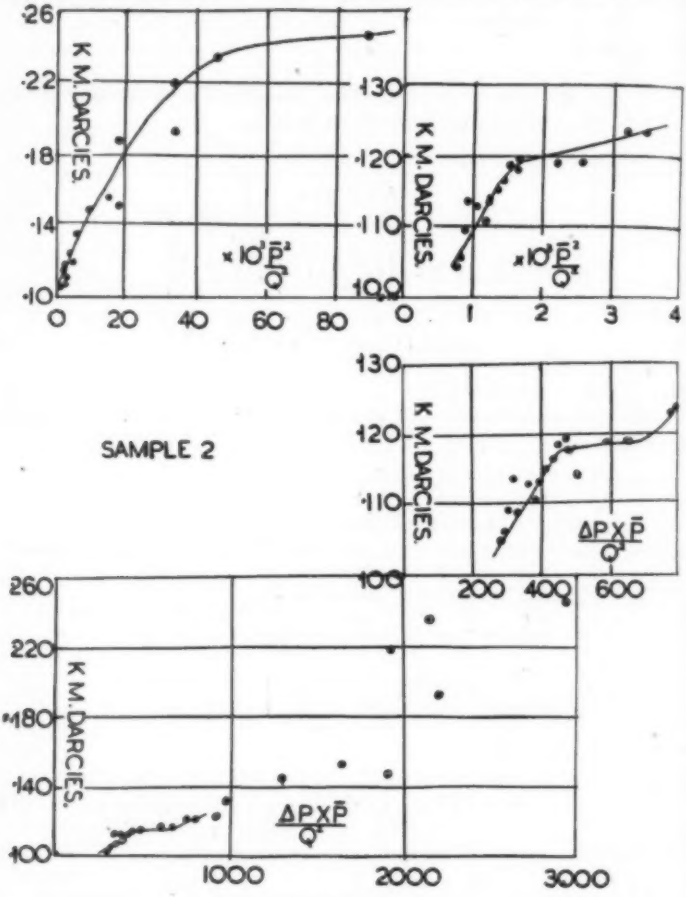

FIGS. 21A AND 21B.

are similar. Where there is spread in the points, the accuracy of measurements was lowest.

Sample 7 (Fig. 29) shows K as a function of $\frac{\bar{P}^2}{Qa^2}$ and of $\frac{\Delta \bar{P} \times P}{Qa^2}$, over part of the range of observations. Again there is a portion of the plot where no curve can be drawn, and this portion is of lowest experimental accuracy.

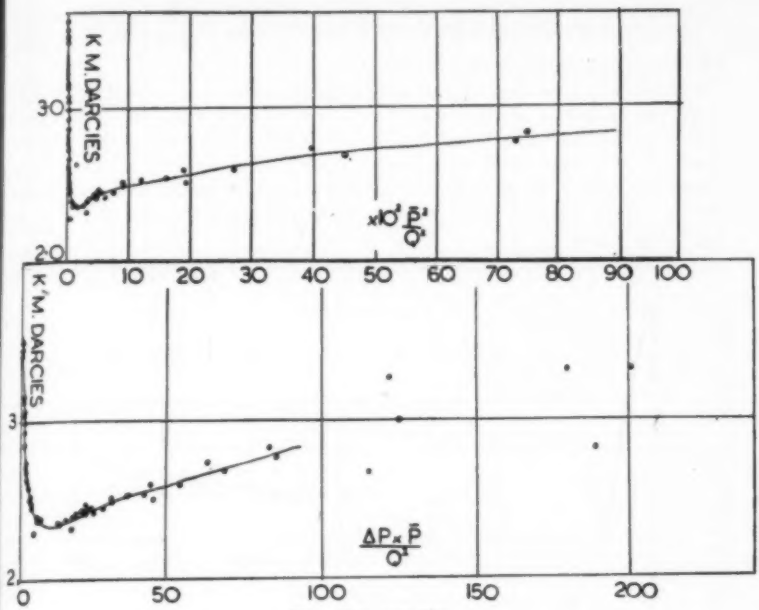

FIGS. 22A AND 22B.

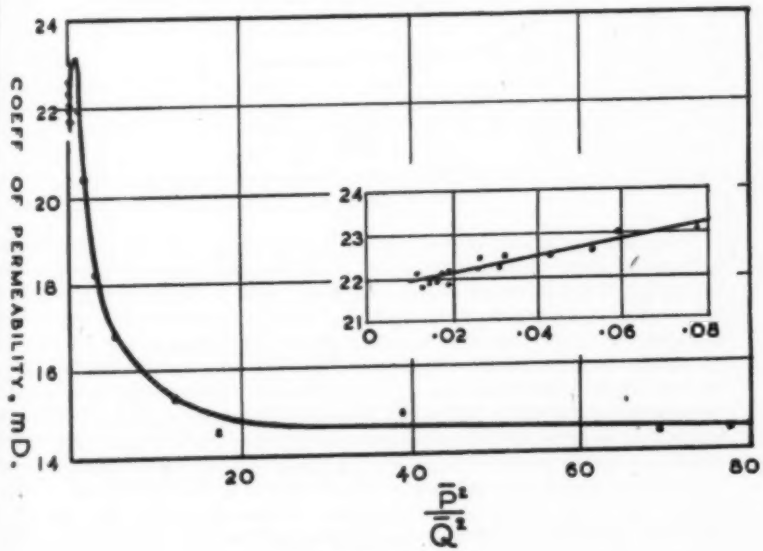

FIG. 23A.

Sample 8 (Figs. 23A and 23B) shows K as a function of $\frac{\bar{P}^2}{Qa^2}$ and of $\frac{\Delta P \times \bar{P}}{Qa^2}$ over the whole range of observations.

At first sight these results may appear inconsistent, because all the samples being porous media, should show a similar variation of the different factors, differing only in degree, but not in fundamentals. It is quite possible, however, that samples 2 and 7 are showing only sections of the general curve exemplified by sample 8. The other samples fall into line with these three. There are still minor differences in the general shape of the curves to be explained.

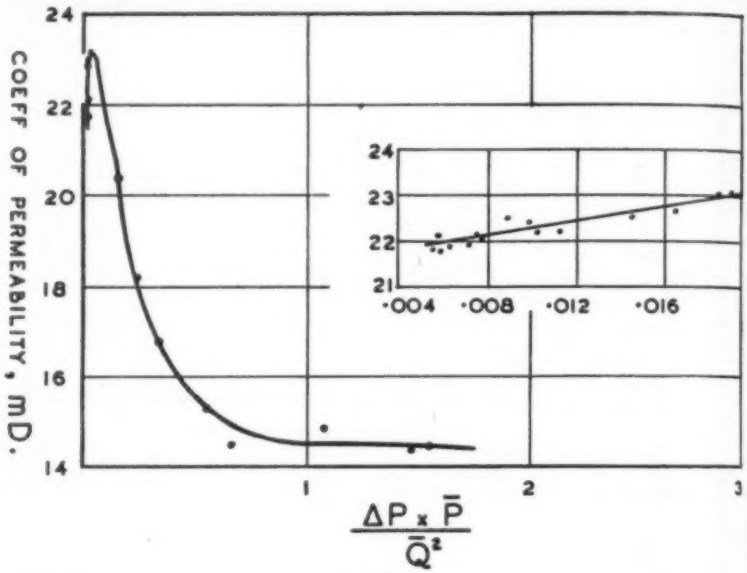

FIG. 23B.

Porous media, whatever their chemical properties, have been assumed to behave similarly, so long as the shape of the channels through which flow is taking place does not alter with the flow. It is to be remembered that porous media are made up of different chemical substances, and should therefore be suspected of influencing flow in different ways. Activated charcoal, for instance, would profoundly affect the hydrodynamical laws of flow when used merely as a porous conduit. Other substances would show different degrees of influence. They adsorb the flowing fluid to different extents, and even the effective diameter in which flow would take place would not be the same for different conditions of pressure, temperature, etc.

M. W. Capek [8] investigated the amount of air adsorbed on Al_2O_3, Fe_2O_3, SiO_2, and other materials which frequently enter into the composition of rocks, and found that the amount of air adsorbed is quite considerable.

Adsorption of gases depends on pressure. It is therefore possible that adsorptive effects interfere with normal hydrodynamic flow, giving a variation of the coefficient of permeability with the functions $\phi_1\left(\frac{\bar{P}^2}{Qa^2}\right)$ and $\phi_2\left(\frac{P \times \bar{P}}{Qa^2}\right)$, or rather with the dimensionless and more fundamental criteria $\left(\frac{\bar{P}}{\rho v^2}\right)$ and $\left(\frac{\Delta P}{\rho v^2}\right)$. Finally, the third function ϕ_3, $\left(\frac{\mu}{vD\rho}\right)$ was considered. This is Reynolds' criterion, which is believed to determine the nature of flow in porous media under different conditions. It is known that within the ordinary range of the viscous region K is invariant with $\left(\frac{\mu}{vD\rho}\right)$. As the flow was very slow, however, it is pertinent to assume that K is a function of $\left(\frac{\mu}{vD\rho}\right)$.

$$K = f\left(\frac{\mu}{vD\rho}\right) = f\left(\frac{\mu}{\bar{D}} \times \frac{1}{v\rho}\right)$$

$$= f\left(\frac{\mu}{\bar{D}} \times \frac{1}{\frac{vaPa}{\bar{P}} \times \frac{\rho a \bar{P}}{Pa}}\right)$$

$$= f\frac{\mu}{\bar{D}} \times \frac{1}{va\rho a} \quad . \quad . \quad . \quad . \quad . \quad . \quad . \quad . \quad . \quad (15)$$

Since $\frac{\mu}{\rho a}$ is constant, it may be written :

$$K = Cf\left(\frac{1}{\bar{D}va}\right) = C'f\left(\frac{D}{Qa}\right) = C''f\left(\frac{Qa}{\bar{D}}\right) \quad . \quad . \quad . \quad (16)$$

It was impossible to evaluate D for the rock samples. Even if this should have been possible by the method used for the Jena glass filter, the variation in pore size would have been too great to allow any conclusion to be reached. It was therefore thought advisable to evaluate the correct values of

$$\frac{vD\rho}{\mu}$$

for the Jena glass filter plotting it *vs.* K. This gave a curve showing a maximum. It was then assumed that an average value of D existed for every sample and that this value was constant for every sample. Thus, plotting Qa *vs.* K for every sample, curves were obtained showing a minimum and a maximum. It was then assumed that the maximum obtained with the rock samples occurred at the same value of Reynolds' number as that for the glass filter. Thus the permeability function of the rock samples were plotted on the same chart as that of the rock samples, so that the maxima were below each other. Fig. 24 shows the similarity of the curves thus obtained.

It may therefore be assumed that a general curve exists on which the coefficient of permeability drops to a minimum at a value of Reynolds'

criterion of about 0·2, rising to a maximum at a value of Reynolds' criterion between 1 and 2 (taking the parameter for length the mean diameter of the pores). For higher values of Reynolds' criterion the value of K becomes more and more independent of the criterion, assuming a constant value, which would correspond to true viscous flow. It may therefore be concluded that there is the probability of the existence of a regime of *subviscous flow* for gases, where the relationship between the pressure drop and the velocity of flow is not governed by the simple linear equation of

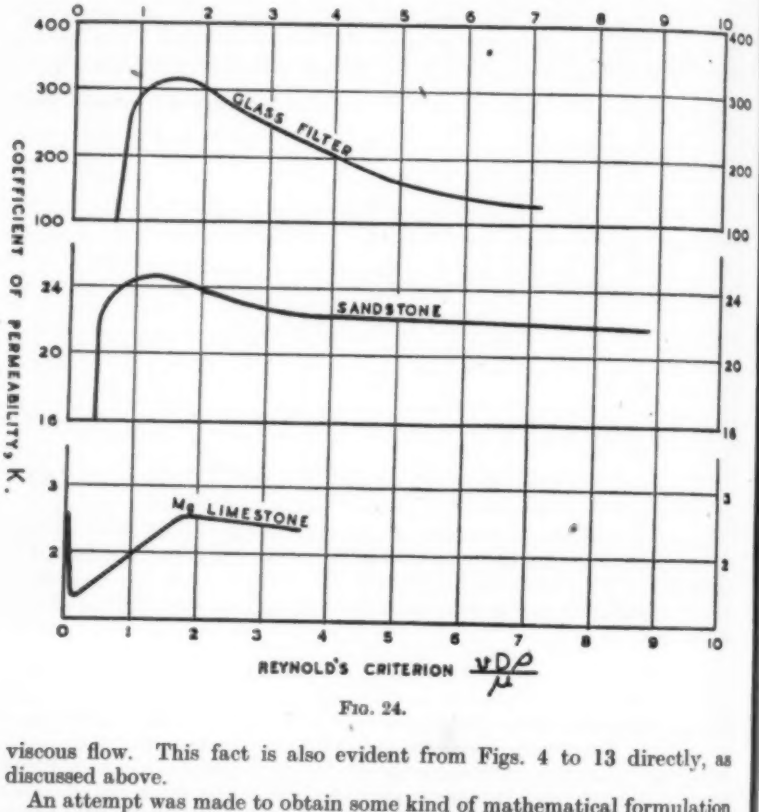

FIG. 24.

viscous flow. This fact is also evident from Figs. 4 to 13 directly, as discussed above.

An attempt was made to obtain some kind of mathematical formulation connecting the pressure drop with the velocity of flow.

An increase of permeability could only be expressed by the presence of a fractional power of v in the permeability equation. Examining the lower portions of the curves of samples 7–9, on which the increase of permeability is quite conspicuous, they were found to approximate to

$$\frac{P}{m} = av^{0.85} \quad . \quad . \quad . \quad . \quad . \quad . \quad . \quad (17)$$

where a was a constant.

The equation for the whole curve was then determined by graphical methods, and found to approximate to

$$P = av^{0.90} + bv + cv^2 \quad . \quad . \quad . \quad . \quad . \quad (18)$$

An attempt to apply this equation to samples 1–6 failed. It is, however, important to mention that these also failed to obey equation 9, *i.e.*:

$$\frac{dp}{dx} = av + bv^2.$$

The fact that maxima and minima are obtained for small values of Reynolds' number is of importance for pressure conservation in gas-wells, as the ratio of yield to pressure drop may be as much as 100 per cent. higher at the maximum permeability than for slightly lower or appreciably higher values of Reynolds' number. Calculations show that the linear velocity in the formation around gas-wells is very small. In a gas-well producing one million cubic feet per day measured at atmospheric pressure, from a stratum 30 feet thick with a borehole of 6 inches diameter, the linear velocity of the gas at the sand face is as low as 3·75 cm. per second at atmospheric pressure. At a distance of 2 feet from the centre of the well the velocity is 0·94 cm. per second, and at 10 feet from the centre of the well the velocity is 0·19 cm. per second. At the higher pressures prevailing in the formation the actual mean linear speeds are smaller than these values. Considering the small pore diameters in the formation and the small linear velocity, the values of Reynolds' numbers under which production is taking place are very small. As the actual calculation of Reynolds' number presents some difficulties, it may be sufficient to use the volumetric rate per unit area of sand face and at prevailing pressures to obtain a value of permeability in tests designed to determine optimum rates of flow.

To summarize: For higher values of Reynolds' number, but below turbulence, the permeability of porous media to gases assumes a constant value which is in accordance with the conditions of viscous flow. For low values of Reynolds' number the existence of a sub-viscous regime of flow for gases must be assumed. It is probable that flow in gas reservoirs is ordinarily in the sub-viscous regime for the major portion of the reservoir. Thus tests should be performed with due regard to the regime obtaining in the reservoir.

Discussion on the Flow of Aqueous Solutions through the Jena Glass Filter.

The flow of aqueous solutions showed that the existence of the sub-viscous regime could not be established in the case of liquids. The curve Q *vs.* P was a straight line, although some deviation could be observed for each solution. There remained to be found whether the adsorptive effects which had been assumed in the case of gases existed for liquids.

The coefficients of permeability were different for the different liquids; further, for each liquid, K showed a variation with temperature. This fact is brought out by Fig. 25, on which the coefficient of permeability to different solutions is plotted against the temperature. It can be seen from the graph that every solution gave a straight line with a definite slope to the horizontal. As the viscosity had already been considered in calculating

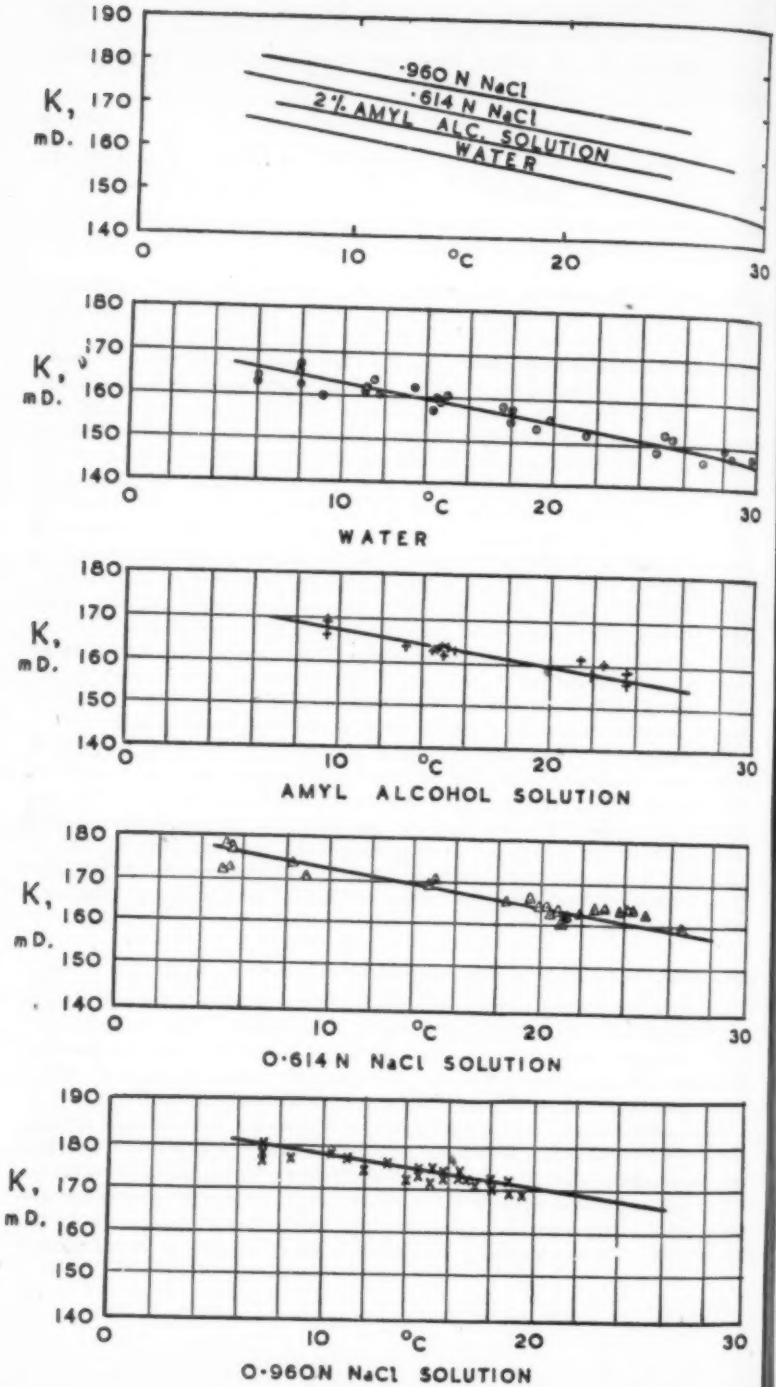
·960 N NaCl
·614 N NaCl
2% AMYL ALC. SOLUTION
WATER
K, mD.
°C
WATER
AMYL ALCOHOL SOLUTION
0·614 N NaCl SOLUTION
0·960N NaCl SOLUTION

FIG. 25.

the coefficient of permeability, it was postulated that the viscosity was not the only property influencing flow.

The conclusion reached was that the effective cross-section under viscous flow was different for different liquids, due to differences in surface energy and consequent differences in thickness of adsorbed layers. As the pressure drop varied with a high power of the radius, small differences in the thickness of these layers could account for the variation in K observed.

A physical interpretation of this fact may be obtained by dimensional analysis. It may be assumed that instead of the viscosity being the sole criterion as a property of liquids governing flow, viscosity μ, density ρ, and the product of surface tension and the average pore diameter d, are all important. Then a dimensionless function obtained is :

$$\left(\frac{\mu^2}{\rho(\sigma d)}\right)$$

As d is a constant for each rock sample, and is unknown for different samples, it is omitted from the criterion. Thus :

$$K = f\left(\frac{\mu^2}{\rho\sigma}\right) \quad . \quad . \quad . \quad . \quad . \quad . \quad . \quad . \quad (19)$$

It is to be remembered that this function is only dimensionless when the product (σd) is used to derive it. No dimensionless function can be obtained from μ, ρ and σ alone.

It is found experimentally that :

$$\log K = \log K_1 + 0{\cdot}1 \log\left(\frac{\mu^2}{\rho\sigma}\right) \quad . \quad . \quad . \quad . \quad (20)$$

Thus the dimensions of K_1 are those of K. To render the equation dimensionless in both variables, K and $f\left(\frac{\mu^2}{\rho\sigma}\right)$,

$$\log\left(\frac{K}{K_1}\right) = 0{\cdot}1 \log\left(\frac{\mu^2}{\rho\sigma}\right) \quad . \quad . \quad . \quad . \quad . \quad (21)$$

Fig. 26 gives the plot for this equation, and it is seen that all four liquids yield points falling on a single curve. The function is in reality $\left(\frac{\mu}{\rho} \cdot \mu \cdot \frac{1}{\sigma d}\right)$, and thus may be taken as the ratio of resistance due to kinematic and absolute viscosity to that due to surface-energy effects. K is then a measure of permeability as governed mostly by viscosity phenomena, and K_1 of permeability as governed by surface energy. In other words, where μ and $\frac{\mu}{\rho}$ are small and σ is large, flow is affected to a greater extent by surface-energy effects than in cases where μ and $\frac{\mu}{\rho}$ are large and σ is small. This is in accord with ordinary experience.

It was concluded that the coefficient of permeability assumes different values with different liquids, and is also dependent on the temperature for each liquid. The slope of the graphs of K *vs.* temperature in degrees

Centigrade is the same for all the liquids tested and is equal to 0·80 *md*/° C. Thus:

$$k = a - b\,(t^\circ\,\text{C.})$$
$$= a - 0{\cdot}80\,(t) \quad . \quad . \quad . \quad . \quad . \quad . \quad . \quad (22)$$

where a is a characteristic constant of the liquid used. It is to be noted that if this equation is the same for all liquids and media used, then from a determination of permeability of a medium to a particular liquid at a single

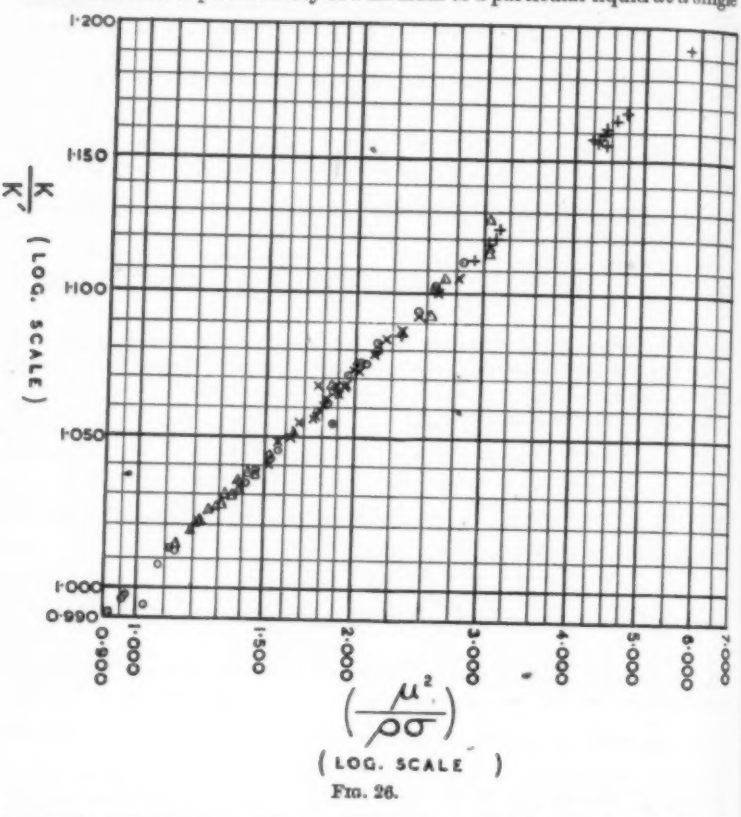

FIG. 26.

temperature the permeability at other temperatures can be calculated. Further work is necessary, however, before this condition can be assumed to be operating.

CONCLUSIONS AND RECOMMENDATIONS.

(1) The permeability of porous media to gases and liquids presents two different problems and in the present work no correlation between these two is apparent.

(2) Permeability to gases is dependent mainly on Reynolds' number, which at small values gives rise to maxima and minima. For higher values of Reynolds' number, but preceding the turbulent regime, permeability assumes a constant value corresponding to viscous conditions. Thus for low rates of gaseous flow in rocks, tests should be carried out at Reynolds' numbers corresponding to those obtaining underground. The "Reynolds' number" may be taken simply as the volumetric rate of flow per unit area of sand, the area being perpendicular to the main line of flow. In other words, the mean linear speed of the gas is taken as the "Reynolds' number." It is further recommended that tests be carried out under a mean pressure equal to that existing underground.

(3) Permeability to liquids is dependent not only on the viscosity, but also on other properties of the liquid which cause a variation in the effective cross-section of the pores under viscous flow. The coefficient of permeability assumes different values for different liquids having different surface-tension values. A single curve was obtained for the different liquid used by plotting against the criterion $\left(\frac{\mu^2}{\rho\sigma}\right)$. The permeability also varies with the temperature for the same liquid, but a correction for this can be obtained for each liquid :

$$K = a - b\,t^\circ \text{ C.}$$
$$= a_1 - b_1\,t^\circ \text{ F.}$$

Further work is necessary before these equations can be taken as universal. The effects of the temperature are fully accounted for in the criterion $\left(\frac{\mu^2}{\rho\sigma}\right)$. Thus for correlation between different liquids at different temperatures this criterion should be used. For correlation with the same liquid at different temperatures the more specific temperature equation may be used.

Department of Oil Engineering and Refining,
University of Birmingham.

Bibliography.

[1] Muskat, M., "Flow of Homogeneous Fluids through Porous Media" (McGraw-Hill, 1937), Ch. II.
[2] Forchheimer, Ph., *Zeits v. deutsch. Ing.*, 1901, **45**, 1781.
[3] Forchheimer, Ph., *loc. cit.*, also "Hydraulik," 1930, 3rd ed., p. 54.
[4] Nissan, Wood, Clark, Nash, *J. Inst. Pet. Techn.*, 1938, **24**, 370.
[5] Muskat, M., "Flow of Homogeneous Fluids through Porous Media" (McGraw-Hill, 1937), p. 681.
[6] L. J. Klinkenberg, "The Permeability of Porous Media to Liquids and Gases." Paper presented to the A.P.I. on 22nd May, 1941.
[7] Buckingham, "Model Experiments and the Form of Empirical Equations." *T.A.S.M.E.*, **37**, 263–296.
[8] *Kolloid. Z.*, 1934, **67**, 145.

THE PHASE TRANSFORMATIONS OF NORMAL PARAFFINS.

By C. G. Gray, B.Sc., A.H.-W.C., A.I.C.

Introduction.

In recent years a considerable amount of information has been published on the crystalline habits of normal paraffins and other long-chain compounds. These studies have shown that polymorphism is common in such compounds, and that crystalline transitions frequently occur in the solid phase. The solid phase transitions have been studied in some detail by various experimenters, each working with a more or less restricted range of compounds, but no attempt appears to have been made to correlate the results observed in these restricted zones and to form a complete picture of the solid phase relationships for a given class of compound. This task is attempted for the normal paraffins in the present paper.

The study of the solid phase relationships in the normal paraffins throws some interesting light on a number of difficulties and apparent inconsistencies in the literature on the crystallography of petroleum waxes. The crystallography of the pure *n*-paraffins is in itself a subject of some complexity; it is therefore not surprising that the interpretation of results on commercial waxes is full of pitfalls.

The Crystalline Modifications of Normal Paraffins.

Pure normal paraffins are known to crystallize in at least four distinct modifications :—

(1) *Hexagonal System*, the hydrocarbon molecules being packed side by side "like hexagonal pencils" (Müller), the long axes being perpendicular to the planes containing the ends of the molecules. This is shown diagrammatically in Fig. 1*a*. The molecules rotate freely about their long axes.

(2) *Orthorhombic System* (Fig. 1*b*). In this modification the molecules are packed side by side perpendicular to the planes containing their ends, *i.e.* the (001) planes, but the packing is no longer hexagonally symmetrical. Two unequal side spacings are shown. The molecules do not possess freedom of rotation, but show libration about their mean positions.

(3) *System uncertain* (monoclinic or triclinic). Two unequal side packing spaces are shown, and the molecules are tilted at an angle of 73° to the planes containing their ends (Fig. 1*c*).

(4) *System uncertain* (monoclinic or triclinic). Two unequal side spacings are shown, and the molecules are tilted at an angle of 61° 30′ to the planes on which their ends are situated (Fig. 1*d*).

In the literature, a great deal of confusion exists over the nomenclature of these four modifications. In the subsequent discussion, the following

nomenclature will be used throughout, and it is suggested that it would provide a convenient standard notation :—

α form : Vertical rotating chains (hexagonal).
β form : Vertical non-rotating chains (orthorhombic).
γ form : chains tilted 73° to (001) planes.
δ form : chains tilted 61° 30′ to (001) planes.

The various crystalline modifications described above are not observed in all normal paraffins, the crystalline habit being governed by the number

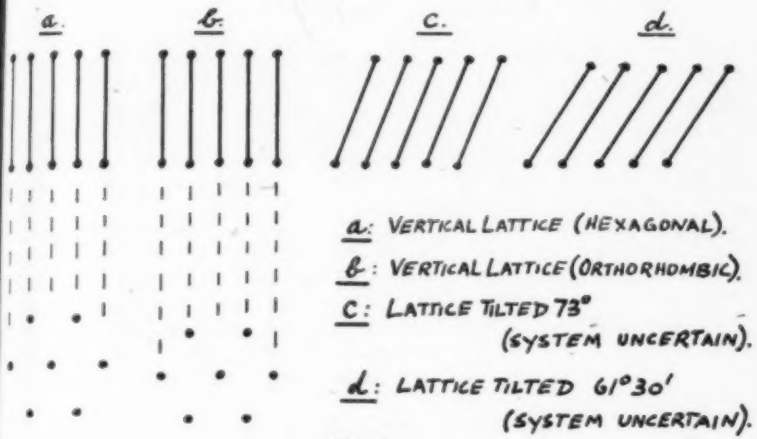

FIG. 1.

CRYSTAL SYSTEMS OF NORMAL PARAFFINS.

of carbon atoms in the molecule. The ranges of n in which each modification has so far been observed are as follows :—

α : Odd paraffins from C_{11} upwards; even from C_{18} upwards.
β : Odd from C_{11} upwards; even from C_{18} upwards.
γ : Odd from C_5 to C_9 inclusive; even from C_6 to C_{22} inclusive.
δ : Even only, C_{24} to C_{36} inclusive. This modification has been obtained only by crystallization from solvents. It has not been obtained by crystallization of melts or by transition from one of the other modifications.

THE MELTING POINTS OF *n*-PARAFFINS.

The melting points of the normal paraffins below C_{20} show odd-even alternation, the values lying on two smooth curves, that of the even members lying above that of the odd. The two curves converge at $n = 20$. Above $n = 20$ the values for both odd and even members lie on one smooth curve. This curve has been assumed to continue up to the highest known paraffins, although erratic values have been found in the region C_{30} to C_{40}.

Theory of Melting.

W. E. Garner and his co-workers have shown that the heats of crystallization of the vertical rotating (α) forms of normal paraffins increase linearly with the number of methylene groups in the molecule.[1] The two terminal methyl groups, on the other hand, contribute a negative quantity to the molecular heat of crystallization. The contributions to the entropy of crystallization are in a similar sense, and it is concluded that "there is a marked tendency for these ends to enter the liquid state."

These facts throw light on the relationship between the melting point and the number of carbon atoms in the molecule for those normal paraffins of which the vertical rotating forms are stable at the melting point.

The latent heat and entropy contributions make it clear that the bonds holding a paraffin molecule in the (vertical) crystal lattice are associated with the (n–2) methylene groups, the terminal methyl groups being repelled by the lattice. When the crystal melts, these (n–2) bonds have to be broken, the energy required being provided by (a) the potential energy of the terminal groups and (b) the vibrational energy of the molecule.

According to the quantum theory of molecular heats, the vibrational energy of the molecule is composed of two separate contributions (a) the energy of vibration of the molecule as a unit and (b) the intramolecular energy of vibration of the atoms within the framework of the molecule. The molecular vibration energy is equal to RT per mole for each degree of vibrational freedom. Taking into account only the energy in the direction parallel to the (n–2) lattice bonds, and distributing this quantity RT equally over these bonds, the contribution to each bond is $RT/(n\text{–}2)$ per mole.

The atomic intramolecular vibration energy is given by Einstein's function $h\nu/e^{\frac{h\nu}{\kappa T}} - 1$, and it is known that except in the region of absolute zero this energy approximates closely to $R(T\text{–}C)$ per mole for each degree of freedom, where C is a constant for a given molecular structure. The total vibrational energy in the direction of the lattice bonds is therefore $R(T\text{–}C) + RT/(n\text{–}2)$ per bond per mole.

The fact that the heats of crystallization of the methylene groups and of the terminal groups respectively are constant above C_8, irrespective of the temperature of crystallization, shows that the bond energy and the potential energy of the terminal groups are constant for similar crystalline forms, irrespective of the temperature of crystallization.

Let the bond energy be E_1 per mole and the potential energy of the methyl groups distributed over the (n–2) bonds, be $2E_2/(n\text{–}2)$ per bond per mole. It is reasonable to assume that at melting, the bond energy is neutralized by the combined potential and vibrational energies, so that

$$E_1 = \frac{2E_2}{(n\text{–}2)} + R(T\text{–}C) + \frac{RT}{(n\text{–}2)}.$$

This equation reduces to the form

$$T = A - B/(n\text{–}1) \text{ where } A, B, \text{ are constants.}$$

Over the range C_{20} to C_{36}, the vertical rotating forms of the n-paraffins

TABLE I.

Melting Points of Normal Paraffin Hydrocarbons.

	n.	M. pt., $t°$ C. (calc.).	M. pt., $t°$ C. (obs.) (2).	$\Delta t°$ C. (calc. minus obs.).
Even: $t = 126{\cdot}81 - \frac{2143{\cdot}41}{n + 3{\cdot}7069}$ (δ form)	6	−94·0	−94·0	0·0
	7	−93·66	−90·05	−3·61
	8	−56·3	−56·8	+0·5
	9	−53·32	−53·69	+0·37
	10	−29·56	−29·72	+0·16
	11	−25·61	−25·61	0·00
Odd: $t = 123{\cdot}7 - \frac{1908{\cdot}86}{n + 1{\cdot}779}$ (α form ?)	12	− 9·65	− 9·65	0·00
	13	− 5·39	− 6	+0·6
	14	+ 5·8	+ 5·5	+0·3
	15	10·0	10	0·0
	16	18·0	18·1	−0·1
	17	22·1	22	+0·1
	18	28·1	28·0	+0·1
	19	31·9	32	−0·1
	20	36·4	36·4	0·0
$t = 123{\cdot}4 - \frac{1659}{n - 1}$ (α form)	21	40·45	40·4	+0·05
	22	44·4	44·4	0·0
	23	48·0	47·4	+0·6
	24	51·3	51·1	+0·2
	25	54·3	53·3	+1·0
	26	57·0	57	0·0
	27	59·6	60	−0·4
	28	62·0	61·6	+0·4
	29	64·1	64	+0·1
	30	66·2	66	+0·2
	31	68·1	68·4	−0·3
	32	69·9	70·3	−0·4
	33	71·6	71·6	0·0
	34	73·1	73	+0·1
	35	74·6	74·6	0·0
	36	76·0	76	0·0
$t = 137{\cdot}4 - \frac{2266{\cdot}7}{n}$ (β form ?)	37	76·1	76·3	−0·2
	38	77·8	77·1, 79·3 *	+0·7
	39	79·3	78·9	+0·4
	40	80·75	80·75	0·00
	41	82·1	80·7, 82·5 *	−0·4
	42	83·4	82·9	+0·5
	43	84·7	83·3, 83·8 *	+0·9
	44	85·9	86·4	−0·5
	50	92·1	92·1, 93·0 *	0·0
	52	93·8	94	−0·2
	54	95·4	95	+0·4
	60	99·6	98·9	+0·7
	62	100·8	100·5	+0·3
	64	102·0	102	0·0
	66	103·1	103·6 †	−0·5
	67	103·6	104·1 †	−0·5
	70	105·02	105·25	−0·23

* Egloff quotes two values without discrimination.
† According to Egloff, "impure."

are stable at the melting point, and the melting points for this range, calculated from the equation $T(°K) = 396{\cdot}4 - \frac{1659}{n-1}$, are shown in Table I,

together with the observed melting points published by Egloff.[2] The constants A and B were evaluated by substituting the observed values of T for C_{22} and C_{36}.

Above C_{36}, and below C_{20}, the values of T calculated from this equation show marked deviations from observed values. It is known that the even paraffins below C_{20} crystallize with tilted chains, the melting point curves of the vertical and tilted forms intersecting at about C_{20}.[3] The odd paraffins above C_9 do not crystallize with tilted chains; nevertheless, the melting point curve of the odd paraffins also shows a discontinuity at

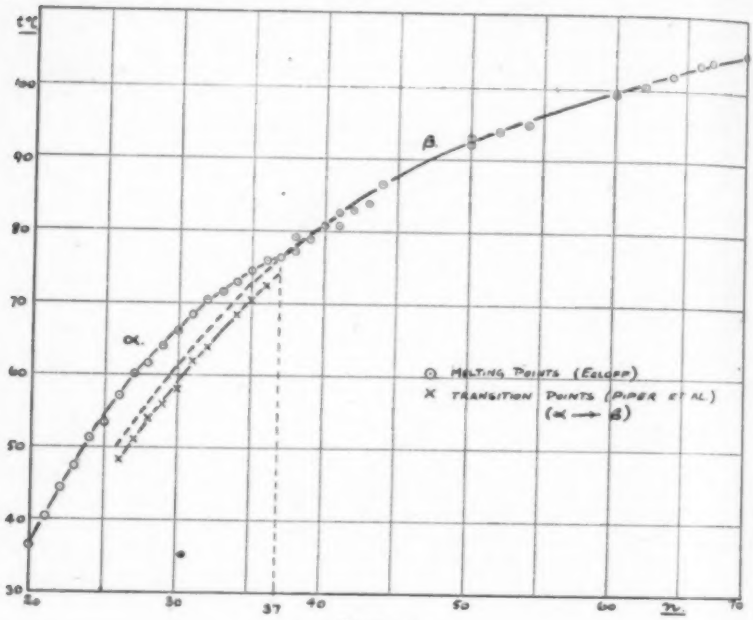

GRAPH 1.

INTERSECTION OF α- AND β-MELTING POINT CURVES AT C_{37}.

about C_{20}. The equations of the "odd" and "even" curves in this zone have been calculated from the observed values, and it has been found that these curves are give by the equations :—

$$T(°K) = 396{\cdot}77 - \frac{1908{\cdot}86}{n + 1{\cdot}779} \quad . \quad . \quad . \quad \text{odd series, } C_{7\text{-}19}.$$

$$T(°K) = 399{\cdot}81 - \frac{2143{\cdot}41}{n + 3{\cdot}7069} \quad . \quad . \quad . \quad \text{even series } C_{6\text{-}20}.$$

The melting points calculated from these equations are compared with observed values in Table I.

The data available on the paraffins with more than thirty-six carbon

atoms in the chain are neither so complete nor so reliable as those for the lower members. Nevertheless it is here suggested that the discontinuity at C_{36} is due to a definite change in the form of crystal which is stable at the melting point above C_{36}. The evidence for this suggestion will appear in the next section. The melting points in the zone above C_{36} lie on the curve: $t° \text{ C.} = 137{\cdot}4 - \frac{2266{\cdot}7}{n}$ as is shown in Table I and in Graph 1.

The Solid Phase Transitions.

The curve for melting point above C_{36} depressed through 2·4° C., continues as a transition in the solid phase for paraffins below C_{37}. The "first transition points on cooling" reported by Piper and his associates [4] for C_{26}–C_{32}, C_{34}–C_{36} are plotted in Graph 1, and are compared in Table II with values calculated from the equation

$$t° \text{ C.} = 135 - \frac{2266{\cdot}7}{n}.$$

Piper and his co-workers confirmed that for paraffins above C_{26} this transition was from the vertical rotating form to the vertical non-rotating form. The tilted forms (angle of tilt 61° 30′) obtained by crystallizing the even paraffins in this range from solvents pass monotropically to the vertical rotating forms, the temperatures at which this takes place laying 0·5–1·5° C. above the "First transition on cooling" line, except for C_{26} and C_{28}, which show a difference of about 3·4° C. between the two transitions.

Table II.

$\alpha \longrightarrow \beta$ Transition Temperatures.

n.	Piper's "transition point, cooling."	Calculated transition point ($\alpha \longrightarrow \beta$) $t° \text{ C.} = 135{\cdot}0 - \frac{2266{\cdot}7}{n}$.	Δt observed minus calculated.
26	48·3	47·8	+0·5
27	51·0	51·0	0·0
28	54·0	54·1	−0·1
29	55·8	56·8	−1·0
30	58·0	59·4	−1·4
31	61·8	61·9	−0·1
32	63·9	64·2	−0·3
34	68·5	68·3	+0·2
35	70·5	70·2	+0·3
36	72·5	72·0	+0·5

Piper's "first transition point on cooling," with the nomenclature adopted in the section on Crystalline Modifications, is the $\alpha \longleftrightarrow \beta$ transition for both odd and even series. The continuity of this $\alpha \longleftrightarrow \beta$ transition line with the melting-point line for paraffins above C_{37} is a strong indication that the β form crystallizes from the melt above C_{37}, and not the α form,

as in the C_{20-37} range. Piper's "transition on heating" at which the δ form passes to α lies a little above the β setting point line in the solid phase, but King and Garner [1] have pointed out that for the longer chains the vertical forms are probably stable at the melting point.

The identification of Piper's "cooling" and "heating" transitions with the $\alpha \longleftrightarrow \beta$ (odd–even) and $\delta \longrightarrow \alpha$ (even) changes, respectively, immediately raises the question of the nature of the transition line which runs roughly parallel to and some 5° C. below the α melting point curve in the range C_{18}–C_{28}, as this line has been assumed to be the line of transition from α to β in this range.[5] This transition has apparently been noted in even paraffins only, no data on odd paraffins in the range having been traced.

Kolvoort [5] and Müller [6] examined the phase transitions of n-$C_{24}H_{50}$, and found that the two transitions, which take place approximately 5° and 10° C. respectively below the melting point, are reversible. On the other hand, the upper transition point in C_{26} and C_{28} is monotropic, as shown by Piper. Above C_{28} this transition does not appear at all. Piper and his associates regarded their sample of triacontane as anomalous in this respect, and continued the curve of the upper transition for C_{26} and C_{28} to join up with those of C_{32} and C_{34}. The evidence available, however, indicates that the upper transition below C_{30} does not correspond with the upper transition in C_{30} and higher hydrocarbons. This is shown in Fig. 2, which shows the observed transition points over the range C_{20}–C_{36}, and the suggested scheme of correspondence between them.

It is perhaps significant that the melting-point curve for C_{36} and over cuts the line of upper transition temperatures for C_{28} and under at the point corresponding to C_{29}, at which point the upper transition (heating) is suddenly depressed (Piper), and is thereafter identified as the ($\delta \longrightarrow \alpha$) transition.

The γ melting-point curve for even paraffins intersects the α melting-point curve at C_{19} approximately,[3] and it is suggested here that the upper transition in the range C_{20}–C_{28} is the continuation of this line as a transition $\alpha \longleftrightarrow \gamma$ for even members. Data on odd members do not appear to be available. The odd members above C_9, however, are not known to exist in a tilted form.

This interpretation is at variance with the conclusions of Kolvoort,[5] who classified the upper transition for n–C_{24} as the point of (enantiotropic) conversion from hexagonal α to orthorhombic β. Kolvoort did not, however, claim to have established the crystalline systems in which his preparations separated. His observations were confined to the angles between the lines of intersection of the (001) and ($hk0$) planes, and were thus incapable of differentiating between vertical and tilted forms. It was assumed that Müller's X-ray data on C_{29} would also be applicable to C_{24}. This assumption, however, is no longer justified.

Müller showed that the lower transition in C_{24} corresponded with the sudden displacement of the (200) reflection in the X-ray spectrum (40–41° C.). Thereafter, with rising temperature, the (200) spacing increased continuously until it became identical with the (110) spacing (46° C.), this being interpreted as a continuous transition of an orthorhombic structure into a radially symmetrical (hexagonal) form in which the chains

are free to rotate. It is, however, possible that the lower transition is from one tilted modification to another (*e.g.* triclinic ⟶ monoclinic), and that the chains do not assume a position vertical to (001) until the upper transition point is reached, at which point the rotation sets in and the molecules take up a vertical position. This point can only be settled

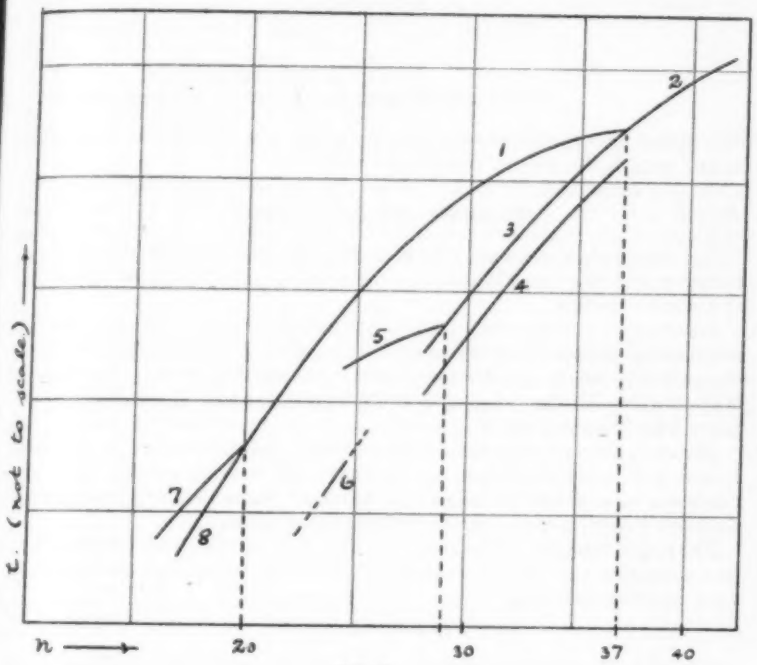

FIG. 2.

PHASE TRANSFORMATIONS OF NORMAL PARAFFINS.

1: α m.pt. (α ⟷ liquid).
2: β m.pt. (β ⟷ liquid).
3: β m.pt. (odd) (β → α).
δ m.pt. (even) (monotropic) (δ → α).
4: β set pt. (odd–even) (α → β).
5: γ m.pt. (enantrotropic below C_{24}) (even) (α ⟷ γ).
6: δ m.pt. (enantrotropic below C_{24}) (even) (γ ⟷ δ).
7: γ m.pt. (even).
8: α m.pt. (odd).

by measurement of the long spacings over the temperature range involved, evidence from short spacings being insufficient to settle the question definitely.

Yannaquis [7] and Bijvoet [8] concluded from X-ray data (the latter on pure *n*–C_{24}) that the upper transition point in this range corresponds with a change from a hexagonal α form to a tilted form. According to Yan-

naquis the tilted form is triclinic; according to Bijvoet it is monoclinic for C_{24}. Bijvoet gives the following scheme for C_{24}.

Hexagonal

↑↓ 46·5° C.

Monoclinic 1

↑↓ 42° C.

Monoclinic 2 (metastable)
or *Triclinic* (stable at room temperatures)

This agrees with the hypothesis that the upper transition for even paraffins in this zone is the $\alpha \longleftrightarrow \gamma$ transition.

Summary and Conclusions.

The equilibrium diagram shown in Fig. 2 is advanced as being in accordance with the available data on the melting and solid-phase transitions of normal paraffins.

Theoretical considerations lead to the formula $T = A - B/(n-1)$ for the relationship between melting point and number of carbon atoms in those n-paraffins in which the α form is stable at the melting point. The formula is applicable over the range $n = 20$–36 inclusive, and is in excellent agreement with observed values.

Above C_{36} the relationship between melting point and number of carbon atoms is of a different type, and the curve for melting point in this zone continues as a transition ($\alpha \longleftrightarrow \beta$) in the solid phase below C_{36}, suggesting that the β form is stable at the melting point above C_{36}.

The upper transition line in the zone C_{20}–C_{28} is probably the continuation, as a transition ($\alpha \longleftrightarrow \gamma$) in the solid phase, of the γ melting-point curve for even paraffins below C_{20}.

Acknowledgment.

Grateful acknowledgment is made by the author to the directors of the Asiatic Petroleum Co., Ltd., and of the Bataafsche Petroleum Maatschapij, for permission to publish this survey.

References.

[1] King and Garner, *J. chem. Soc.*, 1934, 1449 (summarizing paper).
[2] Egloff, "The Physical Constants of Hydrocarbons," A.C.S. Monograph No. 78 (Reinhold Publishing Co.).
[3] Phillips and Mumford, *J. chem. Soc.*, 1934, 1657.
[4] Piper, Chibnall *et al.*, *Biochem. J.*, 1931, **25**, 2072.
[5] Kolvoort, *J. Inst. Petrol.*, 1938, **24**, 338.
[6] Müller, *Proc. roy. Soc.*, 1932, A. **138**, 514.
[7] Yannaquis, *Ann. Comb. Liq.*, 1934, **9**, 295.
[8] Bijvoet, Amsterdam Univ., 1939, unpublished communication to Bataafsche Petroleum Mij.

CALIBRATION OF C.F.R. REFERENCE FUELS.

Calibration of Secondary Reference Fuel F.4 + 4 mls. T.E.L./Imp. Gln. and C.12 + 4 mls. T.E.L./Imp. Gln. by C.F.R. Motor Method I.P. 144/42(T) and the 17° Motor Method I.P. 43/42(T).

Report of Sub-Committee No. 5—Engine Tests.

Aviation Fuel Knock-Rating Panel.

Introduction.

In accordance with standing procedure, the above calibration has been considered on the introduction of F.4 Reference Fuel. As F.4 appeared to be similar to F.3 it was decided to determine whether the calibration for leaded F.3–C.12 would be accurate enough for use with the latest batch.

Tests.

Blends consisting of (50% F.4 + 50% C.12) + 4 mls. T.E.L./I.G.
and (90% F.4 + 10% C.12) + 4 mls. T.E.L./I.G.

were rated in terms of leaded F.3 and C.12 in ten C.F.R. engines by 17° Motor Method. The results of test are given in Table I.

Table I.

C.F.R. Engine.	(50% F.4 in C.12) + 4 mls. T.E.L./I.G. in (% F.3 in C..?) + 4 mls. T.E.L./I.G.		(90% F.4 in C.12) + 4 mls. T.E.L./I.G. in (% F.3 in C.12) + 4 mls. T.E.L./I.G.	
		Diff.		Diff.
A	49·8	−0·2	89·6	−0·6
B	50·3	+0·3	91·0	+0·8
C	52·2 *	+2·2	93·0 *	+2·8
D	50·0	0	90·0	−0·2
E	50·4	+0·4	90·0	−0·2
F	50·3	+0·3	90·3	+0·1
G	49·7	−0·3	90·0	−0·2
H	49·8	−0·2	90·2	0
I	50·0	0	90·0	−0·2
J	50·0	0	91·0	+0·8
Average	50·0	—	90·2	—

* Ratings on Engine "C" have not been included in the average, as they were obviously in error.

Conclusion.

As the average difference is negligible (less than 0·1 O.N.), it is recommended that the calibration tables issued by the Institute of Petroleum for F.3 + 4 mls. T.E.L./I.G. in C.12 + 4 mls. T.E.L./I.G.* shall be employed for leaded F.4 and C.12.

* *J. Inst. Petrol.*, 1941, **27** (211), 192.

The amended Table is reproduced herewith as Table II.

TABLE II.

Octane-Number Calibration Tables C.F.R. Motor Method (I.P. 44/42(T)) up to 100 O.N., thence by "17° Motor Method" (I.P. 43/42(T)).
F.4 + 4 mls. T.E.L./I.G. in C.12 + 4 mls. T.E.L./I.G.

% F.4 + T.E.L.	O.N.	% F.4 + T.E.L.	O.N.
0	93·3	50	103·0
2	93·7	52	103·4
4	94·0	54	103·9
6	94·4	56	104·4
8	94·8	58	104·8
10	95·2	60	105·2
12	95·6	62	105·7
14	96·0	64	106·2
16	96·4	66	106·6
18	96·8	68	107·0
20	97·2	70	107·5
22	97·5	72	108·0
24	97·9	74	108·5
26	98·3	76	109·0
28	98·7	78	109·5
30	99·1	80	110·0
32	99·4	82	110·5
34	99·8	84	111·0
36	100·2	86	111·5
38	100·6	88	112·1
40	101·0	90	112·7
42	101·4	92	113·3
44	101·8	94	114·0
46	102·2	96	114·6
48	102·6	98	115·3
		100	116·0